Palaeogeography, Palaeoclimatology, Palaeoecology 416 (2014) 4–16

Contents lists available at ScienceDirect

Palaeogeography, Palaeoclimatology, Palaeoecology

journal homepage: www.elsevier.com/locate/palaeo

Trace elements and their isotopes in bones and teeth: Diet, environments, diagenesis, and dating of archeological and paleontological samples

Bruno Reynard *, Vincent Balter

Université de Lyon, France
CNRS, France
Ecole Normale Supérieure de Lyon, Site Monod, 15 parvis René Descartes BP7000, Lyon F-69342, France
Université Claude Bernard Lyon 1, 43 Bd du 11 Novembre 1918, F-69622 Villeurbanne Cedex, France

ARTICLE INFO

Article history:
Received 24 March 2014
Received in revised form 10 July 2014
Accepted 31 July 2014
Available online 9 August 2014

Keywords:
Trace elements
Biogenic apatite
Diet
Environment
Diagenesis
Dating

ABSTRACT

Fossil biogenic apatites display trace element (TE) compositions that can record environmental and biological signals, give insights into past water compositions, or be used for dating paleontological and archeological bones and teeth. Processes of TE incorporation into apatites of skeletal phosphatic tissues are described, ranging from those active in living organisms to those active during diagenesis. Abiotic incorporation mechanisms have been modeled theoretically and experimentally and include crystallographic controls on TE partitioning coefficients, inorganic surface adsorption and adsorption mediated through chelation and diffusion–adsorption processes, each leading to specific fractionation patterns. Predictions from models and experiments have been tested against TE concentration and isotopic composition data on remains of contemporary wild or raised animals and on fossils of various ages and environments. In living organisms, TEs incorporated in apatite are separated in two categories, non-essential elements whose concentration is compared to that of an essential element with similar behavior (e.g. Sr/Ca) to reconstruct trophic chains, and essential elements whose isotopic ratios are used to trace metabolic activity, diet, etc. In fossils, elements are incorporated during diagenesis, such as rare earth elements (REEs), and trace diagenetic processes ranging from very early quantitative adsorption likely mediated by chelators, protracted diagenesis through inorganic adsorption and fractionation through diffusion–adsorption, to low-grade metamorphism associated with intense redistribution under crystal-chemical control. These different steps are also identified as steps of radionuclide incorporation. Only samples where the earliest steps can be deciphered are useful for determining stratigraphic and archeological ages. Other samples will date late diagenetic events that have obliterated the paleoenvironmental signals, but may be of geological significance, e.g. tectonic events.

1. Introduction

TEs have long been known to enter bio-apatites of the exo- and endoskeletons of organisms during their life (Stoeltzner, 1908; Hodges et al., 1950) and during the *post mortem* fossilization processes (Arrhenius et al., 1957; Parker and Toots, 1970). Their concentrations and stable isotopic compositions contain information firstly on intensive and extensive parameters of the environment during the life of the organisms, such as temperature, water composition, food and place in the trophic chain, and secondly on conditions, timing and extent of diagenetic alteration of this paleoenvironmental signal. Understanding the mechanisms of TE incorporation and the thermodynamics and kinetics at work during those processes is essential for separating the information pertinent to paleoenvironmental conditions from that relating to the diagenetic history.

Elements like the alkali-earth (Mg, Sr, Ba) are incorporated in significant amounts during life, and divalent metals (Zn, Cu, Fe) at lower levels. These elements will typically be used to trace the environmental and biological signals. Elements like REE and high-field strength elements (Hf, U, Th) are incorporated post-mortem, and trace diagenetic processes from early on in water-rich unconsolidated sediments to low-grade metamorphism. Lu, Th and U are used for dating provided that they can be linked to diagenetic events that took place in a relatively short time interval after the death of the organism.

Different laws govern incorporation of TEs depending on their nature and on the mechanism of uptake by fossils. Properties of the bulk crystal influence the partitioning of TEs with biological or environmental fluids when recrystallization is important during the growth of the skeleton or

* Corresponding author at: Université de Lyon, France. Tel.: +33 4 72 72 81 02; fax: +33 4 72 72 86 77.
E-mail address: bruno.reynard@ens-lyon.fr (B. Reynard).

http://dx.doi.org/10.1016/j.palaeo.2014.07.038
0031-0182/

in case of dissolution–precipitation during fossilization. Interactions with mineral surfaces can also play an important role at each of these stages. Interaction with organic molecules is an overlooked mechanism that may explain features of element partitioning in vivo or at early diagenetic stages when part of the organic fraction of the skeletons is preserved or when fluids are rich in chelating organic agents due to biological activity in soils and sediments.

In addition to the direct crystal-chemical effects, partitioning can occur due to kinetic controls on dissolution, precipitation, and transport of the elements in the complex skeleton structure. This implies a complex interplay of aqueous transport in mesoscale pores, diffusion at wetted grain boundaries, diffusion and concentration-controlled dissolution or precipitation, and buffering or intermittent interaction with the diagenetic fluid. Quantification of these phenomena is essential for deciphering potential alteration of the paleoenvironmental signal and for interpreting ages provided by radiogenic isotopic measurements.

Various incorporation mechanisms lead to specific partitioning and composition patterns in fossils that can be assessed by thermodynamic modeling or experimental investigations. We discuss here theoretical and experimental evidence of activity of these different processes, and their consequences on the interpretation of the fossil record in terms of biological signals, paleoenvironments, dating, and diagenetic processes.

2. Mechanisms of TE incorporation in apatite: theoretical and experimental constrains

2.1. Partitioning between aqueous fluids and crystals

Partitioning of divalent cations is defined by the chemical equilibrium expressing divalent cation (Me^{2+}) exchange between apatite and aqueous solutions:

$$Me^{2+}(aq) + Ca\text{-apatite}(ss) = Ca^{2+}(aq) + Me\text{-apatite}(ss), \quad (1)$$

where (aq) and (ss) refer to the aqueous solution and to the solid solution, respectively, with the associated equilibrium constant:

$$K_D\left(\frac{Me^{2+}}{Ca}\right) = \frac{\frac{X_{Me\text{-apatite}}}{X_{Ca\text{-apatite}}}}{\frac{m_{Me^{2+}}}{m_{Ca}}} = \frac{K(T)_{Ca\text{-apatite}}}{K(T)_{Me\text{-apatite}}}\frac{\lambda_{Ca\text{-apatite}}}{\lambda_{Me\text{-apatite}}}\frac{\gamma_{Me^{2+}}}{\gamma_{Ca}}, \quad (2)$$

where X is the molar fraction in apatite solid solution, m the molality in water, λ the activity coefficient of the component in the solid solution, $K(T)$ the solubility product of the end-member at temperature T, and γ the ion activity in the aqueous solution, whose ratio in water is assumed to be equal to unity in the following. The activity coefficients in a regular solid solution model are described by Margules parameters and can be approximated by the elastic energy due to the deformation of the host crystal lattice around the substituted cation (Brice, 1975):

$$W_{G_{ji}} = 4\pi N_A E\left[\frac{r_i}{2}\left(r_j - r_i\right)^2 + \frac{1}{3}\left(r_j - r_i\right)^3\right], \quad (3)$$

where N_A is the Avogadro number, E the Young's modulus of the crystal, r_i the ionic radius of the cation normally occupying the site in the i compound (Ca in apatite), and r_j the ionic radius of the substituted cation in compound j. Elasticity of hydroxyapatite gives $E = 114 \pm 2$ GPa (Gilmore and Katz, 1982; Bass, 1995). Numerical applications with 6- to 9-fold coordination ionic radii (Shannon, 1976) give similar results. The elastic energy is assumed constant over the pressure and temperature interval of interest. Using slightly different boundary conditions leads to different equations (Nagasawa, 1966; Gnanapragasam and Lewis, 1995) and to differences in the substitutions energies in the order of ±10%. Apatite solid solution properties were also accurately modeled from interatomic and first-principles calculations (Rabone and De Leeuw, 2006; Kawabata and Yamamoto, 2010; Almora-Barrios et al., 2013).

At low concentrations ($X_{Me\text{-apatite}} \ll 1$) like those of TEs in biogenic apatites, Eq. (2) reduces to:

$$K_D\left(\frac{Me^{2+}}{Ca}\right) = \frac{K(T)_{Ca\text{-apatite}}}{K(T)_{Me\text{-apatite}}}\exp\left(-W_{G_{MeCa}}/RT\right) = \exp\left(-\left(G_{ideal} + W_{G_{MeCa}}\right)/RT\right), \quad (4)$$

where the term $\exp(-\Delta G_{ideal}/RT)$ is the free enthalpy change of reaction (1), equivalent to the ratio of end-member solubility products. Unlike carbonates, solubility products and thermodynamic data for end-member apatites are scarce (Jemal et al., 1995). When no data are available for the solubility and enthalpy of formation of the end-members, it is assumed that the elastic energy term dominates partitioning, i.e. $\Delta G_{ideal} \ll W_{G_{MeCa}}$. Promising ways for obtaining enthalpies of formation and substitution energies are first-principles calculations (Almora-Barrios et al., 2013) and atomistic modeling (Rabone and De Leeuw, 2006).

For heterovalent substitutions, the equilibrium reaction becomes complex since complementary substitutions are necessary to maintain charge balance in the crystal. Typically, substitution of the trivalent elements of the important rare-earth series requires compensation by Na^+ for Ca^{2+} in an adjacent site, or yet more complex substitution scheme involving carbonate groups, fluorine (Yi et al., 2013). In that case, most thermodynamic data required for calculating the equilibrium constant are not available. Among a series of elements with the same charge and substitution scheme, the pattern of equilibrium constants, or of distribution coefficients, can be approximated by combining Eqs. (3) and (4) (Blundy and Wood, 1994, 2003):

$$K_D = K_D^0 \exp\left(-4\pi N_A E_{eff}\left[\frac{r_0}{2}\left(r_j - r_0\right)^2 + \frac{1}{3}\left(r_j - r_0\right)^3\right]/RT\right), \quad (8)$$

where E_{eff} is the effective Young's modulus and r_0 is the optimum radius for maximum equilibrium constant K_D^0, all of which will depend on the charge of the considered series of elements. These parameters can be adjusted to experimental data such as partition coefficients between minerals and liquids (Blundy and Wood, 1994) and lead to parabola-like curves whose position and curvature depends on the charge of the element (Fig. 1). This approach was so far only applied to rare-earth elements in apatite (Fig. 2), where relative partition coefficients were extrapolated from magmatic temperatures around 800 °C (Fujimaki, 1986) to low temperatures appropriate to fossil diagenesis (Reynard et al., 1999).

2.2. Surface adsorption, complexation, and chelation

The chemical equilibrium used above applies to systems where solution–precipitation and diffusion in solids are fast enough to allow equilibration between the fluid composition and bulk composition of crystals. This is usually far from being the case in living organisms and in low temperature sedimentary environments. Equilibrium (1) may in this case be replaced by local equilibrium between the ions in solution and ions adsorbed on the apatite surfaces. The crystal surface composition is incorporated in the crystal during its growth with equilibrium constants that can differ strongly from those of equilibrium (1) between a bulk mineral solid solution and aqueous solutions. Direct measurement of surface composition in equilibrium with a fluid is difficult, and few data on surface speciation are available (Rimbert et al., 1982). The thermodynamics of this local equilibrium may be discussed from the difference between effective fractionation as measured on experimentally grown crystals and equilibrium (1). Surface adsorption energies and associated equilibrium constants can be obtained from first-principles calculations that were so far applied to Mg incorporation in

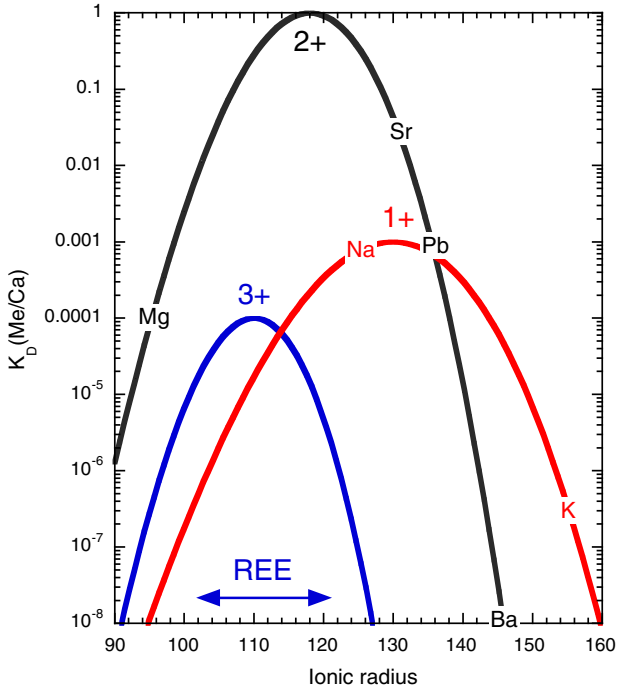

Fig. 1. Crystal-chemical control is illustrated by the effect of ionic radius (shown here for 9-fold coordination) on equilibrium partition coefficients between liquid and crystal for several cation charges (Blundy and Wood, 2003). Curvature and location of maxima may depend on the charge and exact charge compensation mechanism.

apatite (Almora-Barrios et al., 2013). Finally, the kinetics of crystallization and of diffusion from the fluid to the mineral surface may play an important role (Baig et al., 1999; Mayer and Featherstone, 2000; Fulmer et al., 2002; Guidry and Mackenzie, 2003).

In a similar fashion to divalent elements, adsorption on mineral surfaces, as well as complexation with organic compounds in the aqueous fluid (e.g. the biological fluid) plays an important role for REE and other metals (Rimbert et al., 1982; Koeppenkastrop and De Carlo, 1992; Rakovan and Reeder, 1996). Sorption of REE elements on apatite surface yields partition coefficients that also display some degree of crystallographic control (Koeppenkastrop and De Carlo, 1992), but to a smaller extent than intracrystalline substitution (Reynard et al., 1999). Crystallographic control can be fitted with Eq. (8) and yields an effective Young's modulus of about 90 GPa, five times lower than that for intracrystalline substitution (Fig. 2). It is worth noting the small variations of adsorption partition coefficients around the smooth curve defined by fit to Eq. (8) that originate from effects of electronic configuration on partly filled 4*d* orbitals in the ligand field of complexes, crystals and crystal surfaces, known as tetrad effect (Peppard et al., 1969; Nugent, 1970).

Complexation of metal cations in aqueous fluids involves binding with a broad range of molecules from simple inorganic ones (e.g. carbonates, phosphates, sulfates) to complex organic ones (humic acids, amino acids, proteins, enzymes etc.). For molecules with several bonding sites and structural flexibility (e.g. multidentate or chelator), complexation is thermodynamically favored with respect to complexation with several monodentates having one bonding site, a process named chelation. Chelators can be adsorbed on mineral surfaces while remaining complexed to metallic cations. The pattern of partition coefficients associated with this process has been measured for rare-earth elements complexed

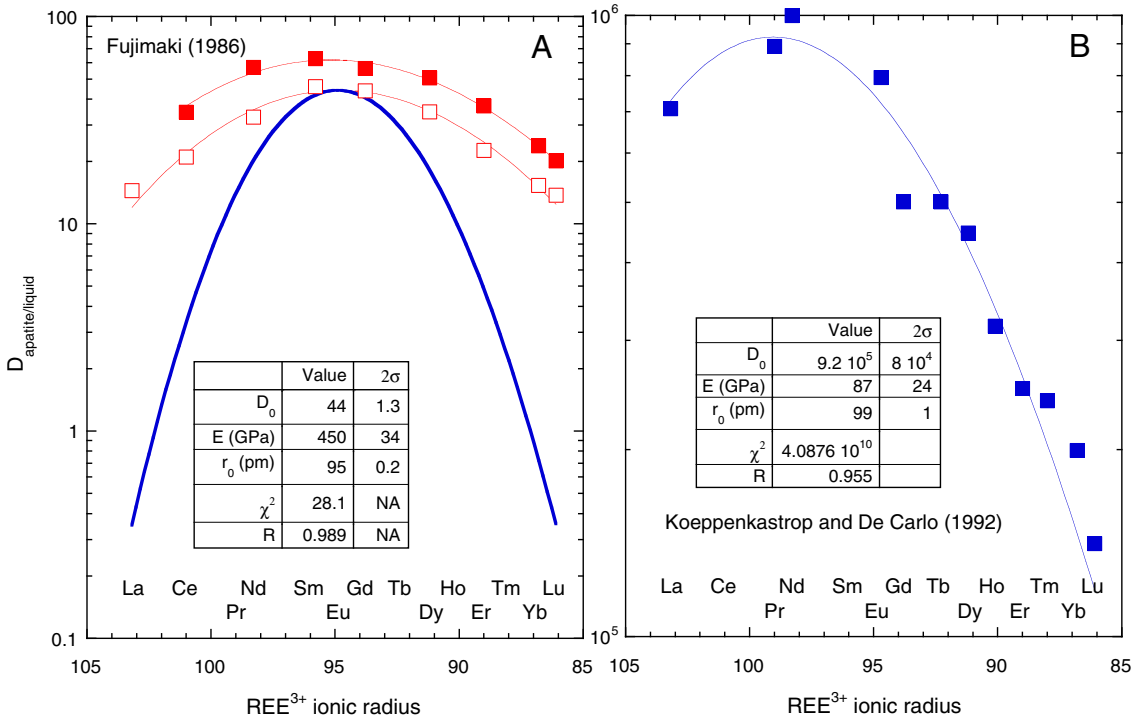

Fig. 2. Fit of Eq. (8) to partition data and ionic radii for 6-fold coordination. A. Patterns of partition coefficient of REE^{3+} between apatite and silicate liquid at high temperature (red symbols) are fitted (red curves) and extrapolated to ambient temperature (blue curve). Extrapolated partition coefficients span more than two orders of magnitude. Maximum partition coefficient is located at 95 pm for an "ideal" radius of 100 pm for Ca. The shift in position of the maximum is due to charge compensation for intracrystalline substitution mechanisms. B. Pattern of partition coefficients for adsorption on apatite surface. Maximum value is observed for a value close to the "ideal" radius of 100 pm, indicating no charge compensation within the structure, but probably in the outer layer at the contact with aqueous solution. Curvature is smaller than for intracrystalline substitution (lower value of E) because of smaller influence of crystal field, and the partition coefficients span slightly less than one order of magnitude. Fluctuations of partition coefficients around the curve are due to tetrad effects. Modified from Reynard et al. (1999).

with humic acids and manganese oxides. It shows null fractionation along the whole series; the effect of chelation is therefore to screen the TE from the crystal or ligand field and to suppress fractionation associated with ionic radius variations and tetrad effects, and most of the anomalies associated with redox of Ce (Davranche et al., 2005). Similar effects might occur for adsorption of chelated metals on other mineral surfaces, and in particular phosphates, but, to our knowledge, this has not been tested in aqueous solutions. Other lines of evidence for a similar effect on bone phosphates comes from treatment bone metastases that makes use of radioactive REE and other metals combined with organic chelators such as ethyldiaminetetramethylenephosphonate (EDTMP), which bind to bones and bone deposition area (Eary et al., 1993; Resche et al., 1997). Systematic tests on mice using different trivalent radionuclides ranging from Ce to Ac (Fig. 3) show that retention on bone is remarkably independent of ionic radius (Beyer et al., 1997). Similar features were observed in bones and in modern bears (Vidaud et al., 2012; Kohn et al., 2013).

In addition to chelators, transition metals also form complexes with proteins and enzymes that interact with bones and teeth in the living organisms and may influence their incorporation in the bio-apatite.

2.3. Diffusion processes

Solid-state diffusion in crystals is a thermally activated process governed by the enthalpy of formation and of migration of defects, and usually well described by the Arrhenius relation:

$$D = D_0 \exp\left(-\frac{\Delta H_a}{RT}\right), \tag{9}$$

where D_0 is a pre-exponential factor corresponding to the diffusion coefficient at infinite temperature, and ΔH_a is the activation enthalpy (or energy) of the diffusion process. Extrapolation of high-temperature diffusion data of TEs in apatite (Cherniak, 2000) shows that these processes are inefficient at temperatures below 300 °C that cover the conditions of diagenetic alteration up to low-grade metamorphism.

Because solid-state diffusion is inefficient during diagenesis, the incorporation of TEs in bones and phosphatic tissues occurs through interactions between mineral surfaces and diagenetic fluids and by solution–precipitation. Conditions range from low-temperatures where these processes can be assisted by biological degradation of the phosphatic tissue to low-grade metamorphism where solution–precipitation with aqueous fluids dominates. The process of TE incorporation comprises several steps, each contributing potentially to fractionation, and depending on the ultrastructure of the bone or tooth.

The porosity structure of the bone or tooth plays an essential role in their incorporation because the transport medium of TEs is solely diagenetic aqueous fluids. There are various hierarchical levels of porosity in bone and teeth (Fig. 4), from large open channels (1–10 μm) of vascularized part of the tissue and open diagenetic cracks, thin cracks associated with channels or interfaces between different parts of the tissue (e.g. at the enamel–dentine junction), to grain boundaries between nano- to micro-metric crystallites of the mineralized tissue. This decreasing scale of porosity is mirrored by an increasing scale of specific area available for TEs incorporation through adsorption and solution–precipitation at cracks and grain boundaries. Thus, the largest potential reservoir for increasing TE content is the geometrically most difficult to reach by diffusion because of its small porosity.

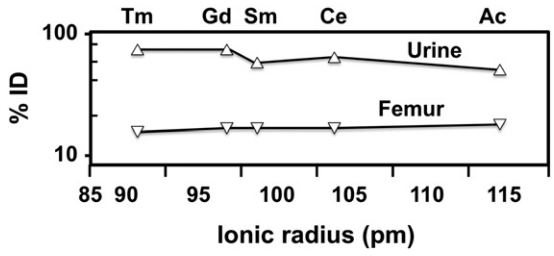

Fig. 3. Concentration of radioactive tracer chelated by EDTMP relative to the injected dose (%ID) in femur and urine of mice as a function of ionic radius for 6-fold coordination (Beyer et al., 1997). The concentration in bone is remarkably independent of ionic radius over a large range that spans REE and beyond (Ac), showing that chelation suppresses the crystal or ligand field effects and results in null relative fractionation of TEs.

Modeling diffusion of dissolved TEs in such a complex porosity structure is non-trivial, and, in the absence of measurements of relevant geometrical and kinetic properties, approximations have been used to reduce the number of parameters required to describe diffusion in the fluid (water) that wets the bones (Millard and Hedges, 1996). Firstly, an effective diffusion coefficient D is defined:

$$D = \frac{D_0 VW}{\tau^2}\left(1-\frac{a}{A}\right)^2\left[1-2.104\frac{a}{A}+2.09\left(\frac{a}{A}\right)^3-0.95\left(\frac{a}{A}\right)^5\right], \tag{10}$$

where D_0 is the diffusion coefficient in the solution, V is the volume porosity, W is the fraction of pore volume filled, τ^2 is the tortuosity factor, a is the hydrodynamic radius of the diffusing species, and A is the radius of the pores assumed cylindrical. Diffusion coefficients in aqueous solution lie typically in the range 2–20 10^{-10} $m^2 \cdot s^{-1}$ at infinite dilution (Yuan-Hui and Gregory, 1974), and a in the range 0.1–1 nm, and A is of the order of 0.8 nm (Holmes et al., 1964). D_0 and a are inversely correlated through the Stokes–Einstein equation. Diffusion coefficients vary with temperature, salinity, and complexation scheme (in particular through variations of a) in complex solutions. With a tortuosity factor of 3 and wetness in the range 0.1–1, the effective diffusion coefficient lies in the range 10^{-11}–10^{-13} $m^2 \cdot s^{-1}$.

With the assumption that only the smallest porosity contributes to diffusion and incorporation of the TE, solutions of the diffusion equation for various geometry can be applied (Crank, 1975) with the effective diffusion coefficient defined in Eq. (10). Assuming a plate-shape for bone and tooth fragments, and an initial concentration C_0 of zero (purely diagenetic tracer such as U, Th or REE), it yields (Millard and Hedges, 1996):

$$C_s = \phi R C_1\left(1-\frac{4}{\pi}\sum_{n=0}^{\infty}\frac{(-1)^n}{2n+1}\exp\left[\frac{-D\left(2n+1\right)^2\pi^2 t\right)}{(R+1)4l^2}\right]\cos\left(\frac{(2n+1)\pi x}{2l}\right)\right), \tag{11}$$

where C_s is the concentration in the solid, C_1 is the concentration in the diagenetic fluid, $R = K_D/p$ is the ratio of the equilibrium constant or partition coefficient K_D to the specific porosity p whose value is in the range 0.1–0.7 10^{-3} $m^3 \cdot kg^{-1}$ (Millard and Hedges, 1996), l is the half thickness of the plate, and x is the distance from exchanging interface along the diffusion profile.

For back-of-the-envelope calculations, it is easy to evaluate characteristic diffusion timescales t from the thickness of the sample and value of the diffusion coefficient (Eq. (10)) from the relation:

$$t \approx l^2/2D, \tag{12}$$

for Brownian motion. With D ~10^{-11}–10^{-13} $m^2 \cdot s^{-1}$ and l from 1 to 10 mm, timescales lie between less than a year and 100 years, i.e. diffusion in the saturating fluid is instantaneous at geological timescales, and nearly instantaneous at archeological timescales. In order to account for simultaneous adsorption during diffusion (diffusion–adsorption or DA model), Eq. (11) is derived from a diffusion equation where the effective diffusion coefficient is the ratio $D/(R+1) \approx D/R$ with R, the fractionation coefficient for adsorption, in the range 10^5–10^7 (Koeppenkastrop and De Carlo, 1992; Millard and Hedges, 1996; Pike et al., 2002). Replacing D by D/R in Eq. (12), typical timescales are in the order of thousands to hundreds of thousand years and account for the observation of diffusion profiles in archeological and geological phosphatic fossils (Kohn, 2008).

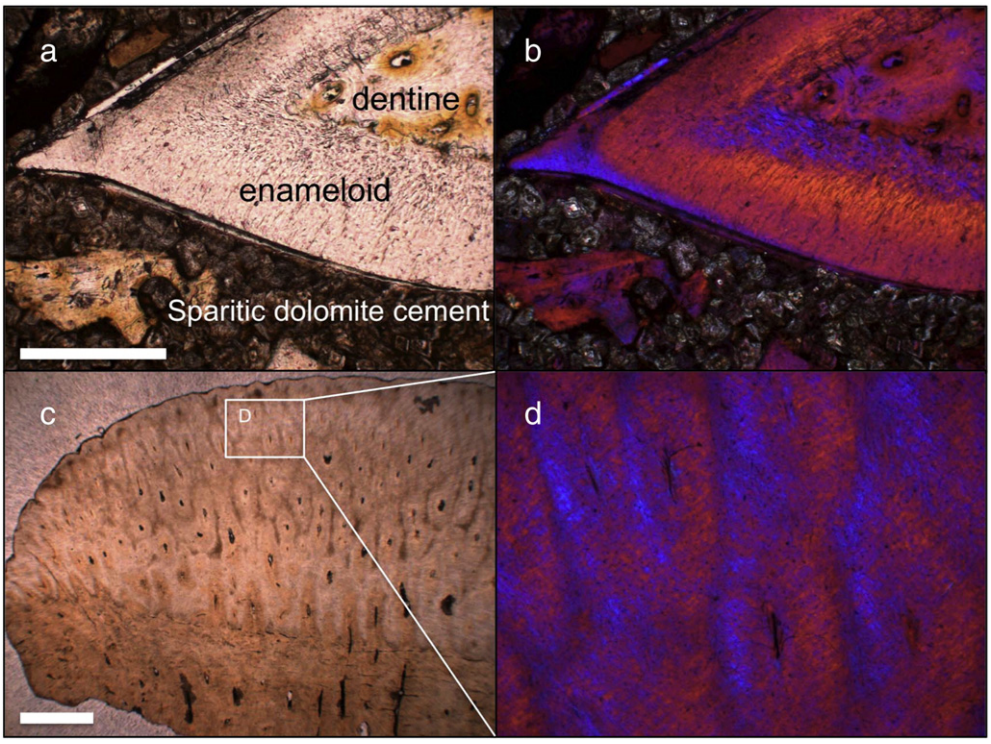

Fig. 4. Examples of phosphatic tissue ultrastructure. a. Polarized light micrograph of a thin section with shark tooth in a phosphatic deposit of the late Cretaceous–Early Paleocene in Egypt showing the densely mineralized enameloid layer, and vascularized, less mineralized dentine tissues. Scale bar is 0.3 mm. b. Same as A with quarter-wave plate and cross-polarizer shows the variability of crystallite orientation in the tissue. c. Polarized light micrograph of a thin section of pycnodont tooth from the Jurassic of Burgundy (France). Note the difference between clear upper part of the tooth, which is heavily mineralized, and the orangey lower part, and the oxide precipitates lining the vascular channels. d. Enlargement of C with quarter-wave plate and cross-polarizer shows the variability and organization of crystallite orientation around the vascular channels filled with oxides. Scale bar is 1 mm.

However, the DA model cannot account for flat U concentrations associated with U-series age gradients, and alternative models of diffusion–recrystallization (DR) or double-medium diffusion (DMD) have been proposed (Kohn, 2008). These involve either a reactive layer or the existence of a disordered boundary layer with higher diffusivity (Stipp et al., 1992) at grain boundaries.

The observation of diffusion concentration profiles can be used to precisely determine timescales if diffusion coefficients are known, or conversely diffusion coefficient if dating is available, through solutions to Eq. (11), or more complex schemes with several stages or mechanisms of TE incorporation (Kohn, 2008). Eq. (11) assumes a platy shape of fossils that may not be appropriate. Assuming one-dimensional diffusion in a semi-infinite medium, one gets:

$$\frac{C}{C_0} = erfc\left(\frac{x}{2\sqrt{Dt}}\right), \tag{13}$$

with x the distance from the bone or tooth edge, C_0 the concentration at $x = 0$ that remains constant, and initial concentration of zero at $x > 0$ (valid for REE and U, Th). It is practical to plot $erfc^{-1}(C/C_0)$ as a function of x, because it gives a straight line with slope $1/\left(2\sqrt{Dt}\right)$ for a given diffusion stage of duration t wherever Eq. (13) applies (Kohn, 2008; Hinz and Kohn, 2010). In this manner, the product Dt may be simply determined. Assumptions or independent determinations are required to constrain either one of the separate variables. Systematic variations of diffusion coefficients in a series of TEs lead to fractionation along the diffusion profile that will add up with fractionation due to variations in partition coefficients. Observed diffusion profiles suggest that the DR and DMD are active mechanisms in enamel with relatively large crystallites, while DA may be more appropriate for dentine and bone with small crystallites (Kohn, 2008; Hinz and Kohn, 2010).

Recent experimental determinations of effective diffusion coefficients in bone in a simulated diagenetic environment suggest slightly lower diffusivities than estimated above for diffusion in solution, a discrepancy attributed to depletion of TEs around bones acting as a sink in sediments, and insignificant fractionation among TE in contradiction with geochemical evidence from natural samples (Kohn and Moses, 2013). Different pathways for diffusion may become available in natural environment, such as microcracks, and supplementary mechanisms may be active. A possibility is that the pH of diagenetic waters is maintained at lower values than in experiments, where it evolves from 7 to 9 within 18 months, favoring solution–precipitation and diffusion at grain boundaries, as assumed in DR and DMD models (Kohn, 2008). Testing these hypotheses should stimulate new experimental studies.

3. TEs in phosphatic tissues of the living organisms

3.1. Biological controls on element intake

The crystallographic structure of apatite allows the incorporation of a wide range of elements at relatively high concentrations (>100 ppm), whatever their ionic radius and charge. However, "living" bone and enamel crystallites do not present high concentrations that are found in fossils for many elements (Arrhenius et al., 1957; Parker and Toots, 1970; Curzon and Cutress, 1983). This is because some elements, mainly heavy and often toxic, do not easily enter the body. For instance, the uptake of REE by the gastro-intestinal tract is difficult because trivalent metal transporters do not exist, contrary to the divalent metal transporter 1 that is active for a variety of metals including Fe^{2+}, Cu^{2+} and Zn^{2+} (Iolascon and De Falco, 2009). However, incorporation of minor amounts (<1 ppm) of various traces, including REE and other high-field strength elements, implies complex biological pathways that are not yet fully understood (Vidaud et al., 2012) and involves direct ingestion of dust and soil (Kohn et al., 2013).

From a paleontological and paleoenvironmental perspective, it is necessary to distinguish non-essential from bioessential elements. Non- and bioessential elements have different fates in the body. Non-essential elements are "passively" processed along some of the biological pathways of an essential element of similar chemical properties, and essential elements are actively involved in biochemical reactions, and pathways, and associated with various organic molecules in the body (e.g. iron with hemoglobin).

Non-toxic elements are absorbed in the gastro-intestinal tract depending on the needs of the body. The chemical composition of the serum, the extracellular milieu, is therefore the result of the balance between the metabolic demands of the organs and the inward flux from the diet. Another important regulation of TE concentrations occurs in osteoblasts and enameloblasts, which are the two specialized types of cells that control the precipitation of apatite crystallites.

The activity of proteins and enzymes involved in bone growth is affected by essential trace metals (Yamaguchi et al., 1986). Zinc stands out as a particularly influent TE in the regulation of bone growth rate (Yamaguchi et al., 1987). Zn-enrichment in the outer enamel with respect to the inner enamel of human teeth (Frank et al., 1989) may be attributed to longer interaction with Zn-bearing enzymes and proteins. Thus, complex organic molecules potentially influence the incorporation of TEs in bio-apatites during life. Enrichment factors between bone and serum (Fig. 5) show that the most enriched TEs in apatite ($>10^3$) are F, Sr and Ba, which are non-essential elements. Lead accumulates in apatite ten times higher than Zn. Both elements have similar chemical characteristics, but the former is clearly heavy and toxic are the latter strongly regulated. Mg, Ni, and Fe display enrichment factors similar to Pb; alkali (Na, K), Se and Cu have similar fractionation close to unity. Although part of the intake may be due to the presence of organically bound metals (Spadaro et al., 1970), the absence of systematic charge effect and, at same charge, of ionic radius dependence indicates that TE incorporation in bio-apatites is not primarily controlled by crystal-chemical effects. Metallo-enzymes and -proteins likely play a significant role in stabilizing transition metals in the fluid with respect to apatite. For alkali and alkali-earth metals, which are not systematically bound to organic compounds, the absence of ionic radius effect may arise from direct complexation on nanocrystalline apatite surface before incorporation in the bulk (Yamaguchi et al., 1987).

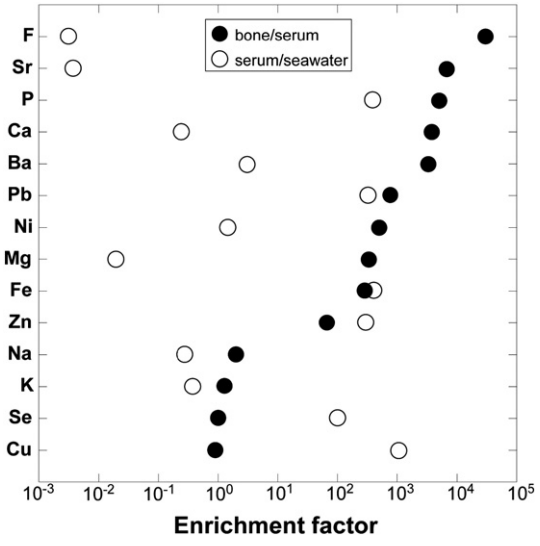

Fig. 5. Enrichment factors for a suite of elements between bone and serum (black dots). Corresponding enrichment factor between serum and seawater is also given for comparison (white dot). Most elements are enriched in bones relative to serum. Concentration data for bone (Hinners et al., 1998), serum (Lyengar, 1989), and for seawater (http://earthref.org/GERM/) were used to calculate enrichment factors.

3.2. Partitioning of non-essential elements

Non-essential elements do not have a recognized vital role in the body but tend to mimic the metabolism of chemically similar bioessential element. The biological behavior of a non-essential element is depicted by using the ratio of its concentration over that of the bioessential element that serves as a reference. This is the case for the Sr and Ba relative to Ca ratios that have been used for over sixty years (Comar et al., 1957; Wasserman et al., 1957), for the less studied Rb/K ratio (Anke and Angelow, 1995; Campbell et al., 2005), and for the Li/Na ratio (Schrauzer, 2002; Kohn et al., 2013). The ratios of non-bioessential elements, e.g. Sr/Ca or Ba/Ca ratios, decrease during the metabolic processes involving the bioessential element Ca, a process often termed biopurification. In healthy adult mammals, biopurification of Ca leads to lower Sr/Ca and Ba/Ca ratios in the body, bones and teeth, than those of the diet. The Sr/Ca and Ba/Ca ratios therefore decrease at each trophic step of a food chain. This was primarily demonstrated for mammal bone (Elias et al., 1982; Gilbert et al., 1994; Burton et al., 1999) and more recently for mammal tooth enamel (Sponheimer and Lee-Thorp, 2006; Austin et al., 2013; Martin et al., 2014), although the type of tissue affects the extent of biopurification (Kohn et al., 2013).

The proportion by which the Sr/Ca and Ba/Ca ratios decrease from one trophic step to the next is constant, and as a result, the two ratios are correlated along a Ca biopurification line (Burton et al., 1999; Balter, 2004). The Sr/Ca and Ba/Ca ratios in bone and enamel of mammals coming from North America are undistinguishable (Burton et al., 1999; Peek and Clementz, 2012), suggesting that the amplitude of the Ca biopurification is similar in bone and enamel, while recent studies showed that dentine was similar to bone and different from enamel (Kohn et al., 2013). Higher Sr incorporation in dentine than in enamel is observed in teeth of mice grown in laboratory and marked with Sr injection (Balter and Reynard, 2008). Since enamel is becoming the material of choice for paleoenvironmental and paleobiological studies, we stress the need for more experimental work linking the Sr/Ca and Ba/Ca ratios in diet, bone and enamel (Peek and Clementz, 2012; Austin et al., 2013). Such studies would be the opportunity to evaluate the scattering the Sr/Ca and Ba/Ca ratios around the Ca biopurification line. Unexpected departure from a Ca biopurification line could serve to identify fossil samples influenced by diagenetic modifications, or contamination with regional rock composition resulting from direct ingestion of dust and soil (Kohn et al., 2013). Coupling of element concentration and isotopic ratio measurements is also a promising line for studying temporal diet evolution and migration of mammals and humans (Balter et al., 2008a,b; Balter et al., 2012).

The reduction of the proportions of Sr and Ba relative to Ca between the diet and the mineralized tissues of an animal is quantified by using Observed Ratio, OR_{Sr} and OR_{Ba}, respectively (Comar et al., 1957), also referred to as Trophic Transfer Factor, TTF (DeForest et al., 2007). For mammals, the values of OR_{Sr} and OR_{Ba} are found quite constant and similar, of 0.30 ± 0.08 and 0.16 ± 0.08, respectively (Balter et al., 2001, 2002a), but can present different values at other sites, and depending slightly on tissues (Kohn et al., 2013), perturbations that may partly be ascribed to contamination by dust ingestion. An OR is an ecological equivalent of a partitioning coefficient and should present temperature dependence. OR_{Sr} and OR_{Ba} are constant for mammals because they are homeotherms regulating their body temperature at 37 °C.

Sr and Ba do partition relative to Ca between synthetic or biogenic apatite and water as a function of temperature (Fig. 6). Experimental Sr and Ba partitioning coefficients were obtained between inorganically precipitated apatite and water, K^{Sr}_{a-w} and K^{Ba}_{a-w} respectively, and decrease when temperature increases (Balter and Lécuyer, 2004). The Sr and Ba partitioning coefficients between bone and enamel of fish raised in controlled conditions and water increase with increasing temperature (Balter and Lecuyer, 2010). Opposite signs of the thermal dependence of K^{Sr}_{a-w} and K^{Ba}_{a-w} are similar to what were observed for some biogenic calcium carbonates (Fig. 7). Using Eq. (4) and thermodynamic data

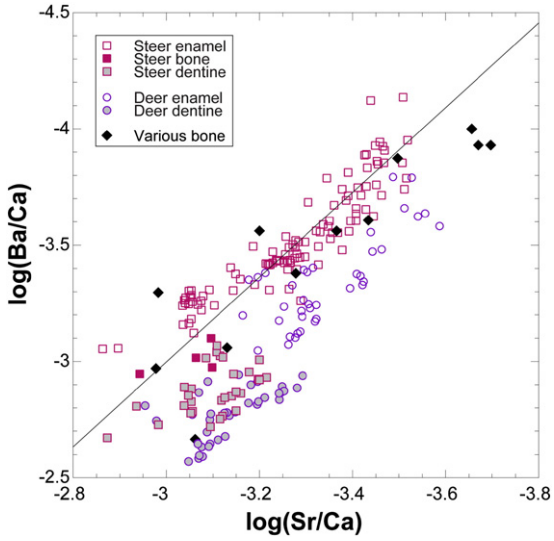

Fig. 6. Sr/Ca and Ba/Ca ratios in enamel, dentine and bone of North American mammals. Steer and deer samples are from Missouri (Peek and Clementz, 2012), and the bone samples (solid diamonds) are from Wisconsin and are represented by several taxa (Burton et al., 1999). The solid line, which represents the Ca biopurification line of the Wisconsin trophic chain (Burton et al., 1999), closely matched the distribution of the Sr/Ca and Ba/Ca ratios in bone and enamel, but not in dentine.

from Jemal et al. (1995), we obtain a range of K_D that spans 4 orders of magnitude, showing that uncertainties on thermodynamic properties are too large to allow discussing equilibrium vs. disequilibrium and biological effects. Thermodynamics implies that partition coefficients tend to 1 at higher temperatures, hence opposite variations are likely due to kinetic or biological control. In the better constrained carbonate system, it has been shown that inorganic precipitation occurs out of equilibrium (Plummer and Busenberg, 1987), while partition systematics of TEs suggest that crystal-chemical controls are dominant during precipitation of some biogenic carbonates (Onuma et al., 1979). Obtaining thermodynamic data from atomistic and DFT simulations should resolve the uncertainties on phosphates and help to better understand TE partition systematics in the complex biological systems.

The sensitivity of K^{Sr}_{a-w} with temperature in bone or enamel is comparable to that of foraminifera and coccolithophorids, suggesting that fossil fish teeth could serve to reconstruct variations of the seawater Sr/Ca composition, provided that the temperature is known independently (Balter et al., 2011). The comparison of the different Cenozoic seawater Sr/Ca records leads to important discrepancies depending on the material used for the reconstruction, i.e. benthic foraminifera, calcite veins, fossil teeth and gastropods (Sosdian et al., 2013). The benthic foraminifera and fish teeth yield similar seawater Sr/Ca records, which are different from those obtained from calcite veins and gastropods (Sosdian et al., 2013). It is tempting to relate this observation to the fact that the equations that relate K^{Sr} to temperature in foraminifera, bone and enamel, have almost identical parameters (Fig. 7). While the Ca metabolism in foraminifera differs strongly from that of vertebrates, the net incorporation of Sr in foraminifera, bone and enamel is fortuitously equivalent. The higher complexity of vertebrates relative to that of foraminifera does not result in a more efficient discrimination against the most abundant elements, and as a whole, our compilation of Sr partitioning in mineralized animals does not reveal clear phylogenetic pattern.

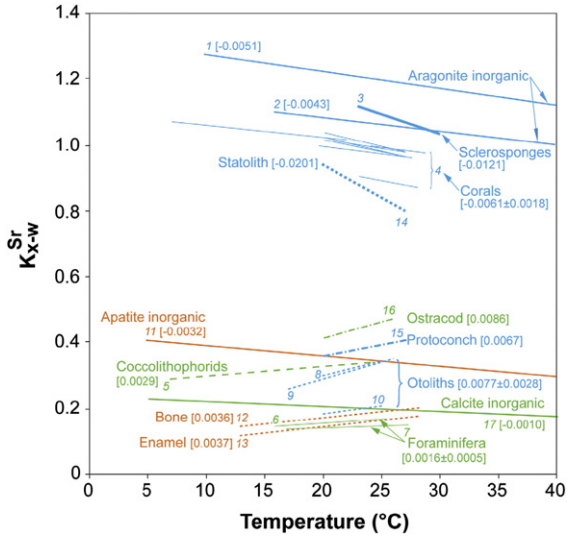

Fig. 7. Temperature dependence of the Sr partitioning coefficient between mineral phases (apatite orange; calcite green; aragonite blue) and water. For a given relationship, the value of the slope is indicated in square brackets and gives the sensitivity of the thermodependence. Data are from: 1, Dietzel et al. (2004); 2, Kinsmann and Holland (1969); 3, Rosenheim et al. (2004); 4, Shen et al. (1996); Cardinal et al. (2001); de Villiers et al. (1994); and Sinclair et al. (1998); 5, Stoll et al. (2002); 6, 7, Lea et al. (1999); 8, Bath et al. (2000); 9, Fowler et al. (1995); 10, Bath-Martin et al. (2004); 11, Balter and Lécuyer (2004); 12, 13, Balter and Lecuyer (2010); 14, 15, Zacherl et al. (2003); and 16, de Deckker et al. (1999).

3.3. Isotopic partitioning of bioessential elements

Bioessential elements have a recognized vital role in the body. Their concentrations are tightly regulated in order to lie between the deficiency and toxicity thresholds. Despite many caveats (Ezzo, 1994; Burton and Price, 2002), this simple rule has often been forgotten in bone-chemistry studies. As such, the concentration of bioessential elements in fossil bones and teeth can potentially be used for tracking paleo-deficiencies or toxicities, at best (Patterson et al., 1987; Rasmussen et al., 2008). In addition, the regulation of a given bioessential element is associated with kinetic processes, changes in the molecular configuration, and redox conditions that are generally associated with isotopic fractionation. This has been early recognized for Ca (Skulan and DePaolo, 1999; Skulan et al., 2007; Heuser and Eisenhauer, 2010), which, although it is the major element of apatite, has rare isotopes that may be regarded as TEs. Isotopic fractionation of Ca is a promising tool for tracing dietary change from bone and tooth compositions (Reynard et al., 2010, 2011, 2013). In this section, however, we will focus here on actual TEs such as Mg, Fe, Cu and Zn, emphasizing isotopic ratios rather than concentrations.

The human body contains about one mole of Mg, of which half is in bone. It is a cofactor for about 300 cellular enzymes and has a pivotal role in energy metabolism (Elin, 1987). Recent study indicated that the Mg isotope composition of enamel is slightly enriched in heavy isotopes relative to bone (Martin et al., 2014), suggesting that a process of preferential segregation of light isotopes is at work during enamel maturation, as in the case of carbon. This study also showed that carnivore bone and tooth enamel are enriched in heavy isotopes relative to those of herbivores, which in turn, do not significantly differ from plants (Fig. 8). The trophic fractionation of Cu is similar to that of Mg, but opposite to that of Fe (Fig. 8), carnivore bone and tooth enamel being depleted in Fe heavy isotopes relative to herbivores and plants (Jaouen et al., 2013). Copper and iron have crucial roles in the transfer of electrons and, consequently, the metabolic relationships between Cu and Fe are multiple (Collins et al., 2010). The Cu and Fe isotopic sex differences that have been first described in blood (Walczyk and von Blanckenburg, 2002; Albarède et al., 2011) have also been shown to be recorded in bone (Jaouen et al., 2012).

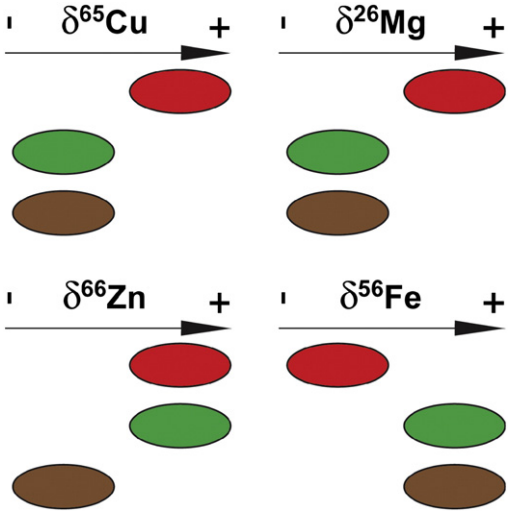

Fig. 8. Schematic distribution of the Mg, Fe, Cu and Zn isotopic ratios in mammal bones and tooth enamel (Jaouen et al., 2013; Martin et al., 2014). Carnivores are in red, herbivores in green and plants in brown.

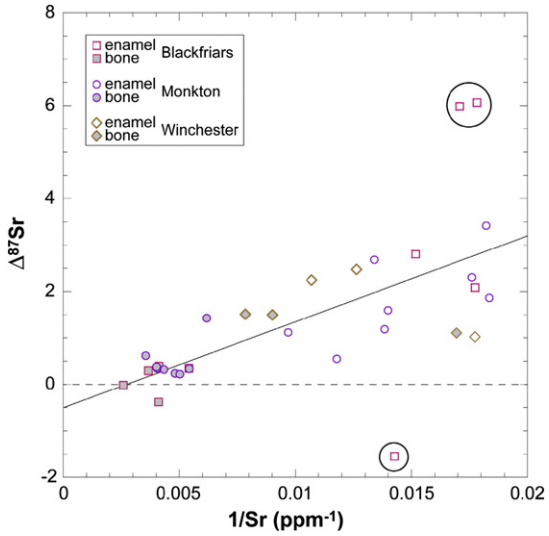

Fig. 9. Relationship between the Sr concentration and the difference between the $^{87}Sr/^{86}Sr$ ($\Delta^{87}Sr$) ratio of the soil and that of the enamel or the dentine in three English archeological sites (Budd et al., 2000). All the samples except those encircled fall on a regression line for which $\Delta^{87}Sr$ tends towards zero (dotted line) when the Sr concentration increases, highlighting the influence of diagenesis. Dentine samples are more altered than enamel samples.

Experimental work is needed to extend to other mammals, especially primates, the potential of the sexing tool based on the Cu and Fe isotope compositions of fossil bone, and possibly fossil tooth enamel. Concerning Zn, a clear trophic fractionation, favoring heavy isotopes, occurs between plants and bones of herbivores (Fig. 8), but not between these latter and those of carnivores (Jaouen et al., 2013). The extent to which isotopic fractionations observed at the trophic scale are a sum of those prevailing in organisms remains unknown. Since pioneering studies, experiments with animals raised on a controlled diet served to calibrate isotopic fractionation factors between trophic steps (DeNiro and Epstein, 1978). The observed depletion of Fe heavy isotopes going up in the food chain (Jaouen et al., 2013) was predicted by animal models (Hotz et al., 2012; Balter et al., 2013) that include segregation against Fe^{3+}, generally enriched in heavy isotopes, during intestinal absorption (Walczyk and von Blanckenburg, 2002).

The picture is more complex for Cu and Zn, because no fractionation is observed between diet and bones in raised animals (Balter et al., 2010, 2013) contrary to observations in wild animals. Differential Cu and Zn uptake, depending on the nature of the diet, i.e. animal vs. vegetal foodstuffs, is presently the preferred explanation to account for this discrepancy (Costas-Rodriguez et al., 2014). The fractionation of isotopes of heavy bioessential elements, often referred to as "non-traditional" isotopes (Costas-Rodriguez et al., 2014), in a biological context is a new avenue of research, which holds great potential for paleobiological applications. Some of the non-traditional isotopes have thus far not been investigated in a biological perspective. This is for instance the case for Si, which is clearly a bioessential element (Schwarz and Milne, 1972), is present in substantial amount (~2.5 g/70 kg) in the body (Iyengar, 1998), possesses its own transporter (Hildebrand et al., 1997), and substitutes for phosphorus in apatites.

3.4. Diagenetic mixing

The measurement of the concentration and isotopic composition of an element that can be incorporated both in the living and *post mortem* in a suite of fossil samples allows testing the existence of a mixing between a biological and a diagenetic pool, provided that these two have different concentrations and isotopic compositions. Various proportions of the diagenetic overprinting result in a correlation between the concentrations and isotope compositions along a mixing hyperbola. If the isotope composition of the diagenetic fluid is known, one can calculate the difference with that of a sample, which must approach zero when the sample has been totally altered (Fig. 9). When possible, the test for a correlation between concentrations and isotope compositions is a powerful method for assessing the extent of diagenesis of a given element in a set of fossil samples. This is routinely done for C and N isotopes in bone collagen and should be the case for Sr and for future analysis of non-traditional isotopes (Jaouen et al., 2012). For Ca, the existence of a mixing equation between concentrations and isotope compositions would rather indicate the persistence of secondary calcite inefficiently removed by acid pretreatments (Balter et al., 2002b).

4. TE incorporation during diagenetic processes and applications

4.1. Incorporation of rare earth and heavy elements

The REE patterns are the signature of the diagenetic processes because in addition to mere concentrations, the relative fractionation among the series is characteristic of the incorporation process. Marine phosphatic remains display a range of patterns that reflect several steps and specific mechanisms of REE uptake from early diagenesis to low-grade metamorphism (Fig. 10). These patterns reflect different diagenetic processes that can be evidenced from a specific combination of REE concentration ratios (Fig. 10; Reynard et al., 1999).

Starting from a low abundance in the phosphatic tissues of the living organisms, REEs are rapidly incorporated *post mortem* in bones and teeth (Arrhenius et al., 1957). REE patterns are, in marine environments, similar to those of seawaters just above the sediment interface (Shaw and Wasserburg, 1985; Elderfield and Pagett, 1986; Elderfield and Sholkovitz, 1987), and in continental environments close to those of groundwaters (Henderson et al., 1983). Concentrations are inversely correlated with crystallite size, suggesting that adsorption on, or diffusion/recrystallization near crystal surfaces is the dominant mechanism (Arrhenius et al., 1957). The absence of large fractionation of REE with respect to ambient waters (Henderson et al., 1983; Elderfield and Pagett, 1986) suggests adsorption of REE as species chelated with organic molecules, e.g. humic acids in soils and similar products of organic matter degradation in marine sediments. Such spectra (PEH3 and NFS5 in Fig. 10) only show constant enrichment factor of about 10^7 with respect to seawater, independent of ionic radius as observed for

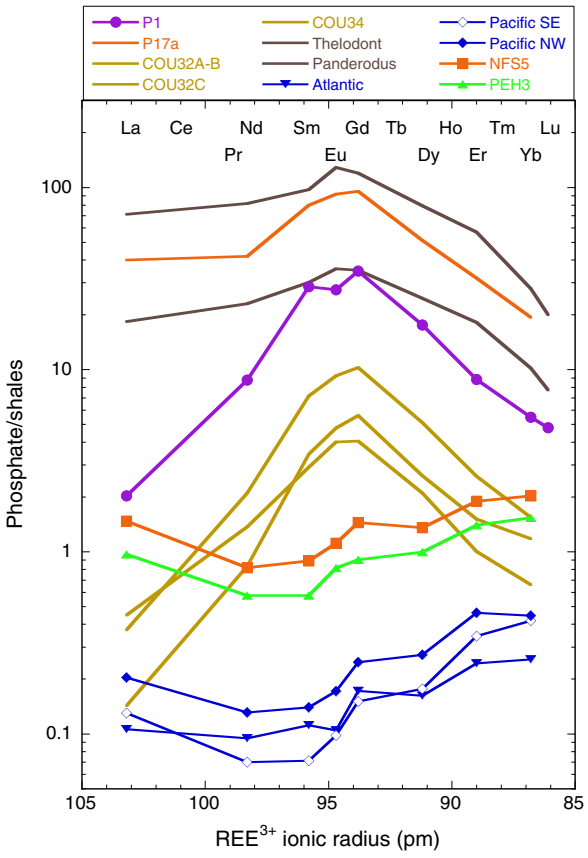

Fig. 10. Selected REE^{3+} patterns in fossil apatites and typical oceanic water spectra for the depth interval 600–2500 m in Atlantic (Elderfield and Greaves, 1982), NW and SE Pacific ocean (De Baar et al., 1983, 1985). All spectra are normalized to the North American Shale Composite (NASC; Gromet et al., 1984) and seawater spectra are multiplied by 10^6 to allow comparison. P1: Triassic fish and P17a Tertiary fish (Grandjean et al., 1987; Grandjean, 1989; Grandjean and Albarède, 1989); COU32-A-B-C, COU34: Devonian conodonts (Grandjean-Lécuyer et al., 1993); Silurian thelodont fish and conodont *Panderodus* (Bertram et al., 1992); NFS5: Tertiary fish (Grandjean et al., 1988); PEH3: Cretaceous marine reptile (Grandjean, 1989).
Modified from Reynard et al. (1999).

chelated REE adsorption on bone (Fig. 3) and humic acid-REE complexes on various minerals (Davranche et al., 2005).

The timescale of the diffusion–advection model discussed above suggests rapid REE uptake, within a few thousand years after sedimentation. This is consistent with the observation that REE concentrations are acquired within the first few millimeters in the sediment and decrease with increasing rates of sedimentation that inhibit REE advection from seawater in the sediment pore waters (Bernat, 1975; Elderfield and Pagett, 1986). In the most oxic sediments, REE patterns are nearly identical to those of seawater, and may be used as paleoenvironmental tracers, whereas in anoxic sediments, strong remobilization of redox sensitive Ce and Eu is observed, along with slight fractionation of heavy REE with respect to seawater, thereby limiting applications to the reconstruction of past seawater compositions (Elderfield and Pagett, 1986).

This mechanism is associated with fractionation and diffusion coefficients that are independent of ionic radius, and diffusion should not induce significant relative fractionation of REE along diffusion profiles, as observed experimentally (Kohn et al., 2013). This may be the case in small fish debris studied in marine environment, but significant fractionation is observed along diffusion profiles in bones from continental and marine environments (Henderson et al., 1983; Trueman and Tuross, 2002; Suarez et al., 2007; Kohn, 2008; Hinz and Kohn, 2010; Kocsis et al., 2010; Suarez et al., 2010; Trueman et al., 2011), suggesting further steps and mechanisms of REE uptake. Perturbation seems especially important in sandstones and clay-rich sediments, where redistribution of the clay signature may buffer the REE pattern (Elderfield and Pagett, 1986; Grandjean et al., 1987; Lecuyer et al., 2004). Contamination by clays was also noted in dating studies using the Lu–Hf system (Barfod et al., 2003) and evidenced by electron microscopy (Kohn et al., 1999).

A second type of REE pattern in phosphatic remains of marine environments is called “hat-shaped”, and shows a moderate enrichment in MREE elements and, to a lesser extent, LREE with respect to seawater (Fig. 10). This pattern is rarely observed in Cenozoic or more recent fossils (Grandjean et al., 1987), but is common in Paleozoic fossils (Wright et al., 1984; Bertram et al., 1992). It is associated with a general increase in REE content, and it may be associated with incorporation through an inorganic adsorption pattern (Fig. 2B), which produces similar, though not identical fractionation (Reynard et al., 1999). The correlation of some characteristics of these REE pattern (e.g. the increase of Sm/Yb ratio) with environmental parameters such as bathymetry led some authors to propose that paleoenvironmental signal and seawater composition may be retrieved from such samples (Picard et al., 2002; Lecuyer et al., 2004). This hypothesis is controversial, and the REE record from carbonate shows no significant evolution from the Cambrian (Shields and Webb, 2004).

In addition to fractionation during adsorption, speciation in water may vary along the REE series, with carbonates competing with chelating agents or organic complexes for association with the heavy REE (Luo and Byrne, 2004; Pourret et al., 2007). This can change the pattern of REE adsorption coefficients on mineral surfaces, as well as the effective diffusion coefficient by changing the hydrodynamic radius of the complexes along the REE series (Eq. (10)). These effects become especially important in continental environments where pH of soil and ground waters are subject to substantial variations of pH at daily, seasonal, and larger timescales. These effects can compound with the regional variability of water composition. This diversity of parameters cannot be constrained from bulk fossil REE patterns alone, and obtaining detailed concentration and isotopic composition profiles proves necessary in order to attempt unraveling the complex diagenetic history of fossils (Henderson et al., 1983; Trueman and Tuross, 2002; Kohn, 2008; Hinz and Kohn, 2010; Kocsis et al., 2010; Trueman et al., 2011).

The third type of REE pattern was called “bell-shaped” because of the large relative enrichment of MREE with respect to both LREE and HREE (Fig. 10). This type of pattern was matched with fractionation patterns under strong crystal-chemical control (Fig. 2A) extrapolated from high-temperature partitioning data (Reynard et al., 1999). It is clearly associated with low-grade metamorphism (<300 °C) that also caused partial graphitization of organic matter in the phosphatic remains (Pucéat et al., 2004). Because solid-state diffusion is inefficient at these temperatures, REE concentrations likely changed through precipitation–solution mechanisms without altering the ornate and delicate shapes of fossils such as conodonts that could still be used for taxonomy (Girard and Albarède, 1996). Similar to the adsorption mechanisms, it is likely that diffusion processes at grain boundaries can induce concentration profiles and enhance or distort the partitioning pattern. For instance, it can be noted that the La/Yb ratio is more affected by low-grade metamorphism (Fig. 11) than expected from the crystal-chemical control alone (Fig. 2A). This may be due either to uncertainties in extrapolation from high-temperature data, or to additional diffusion or speciation effects between LREE and HREE in the metamorphic waters.

Finally, the distinction between the three types of patterns defined here is semantic because the three steps of diagenetic alteration may superpose and contribute to various extents to the REE signature of a single specimen. Diagenetic signatures may be acquired at different steps, from marine environments to soils, during reworking in continental aquifers, and finally during low-grade metamorphism associated with sedimentary burial or tectonic activity.

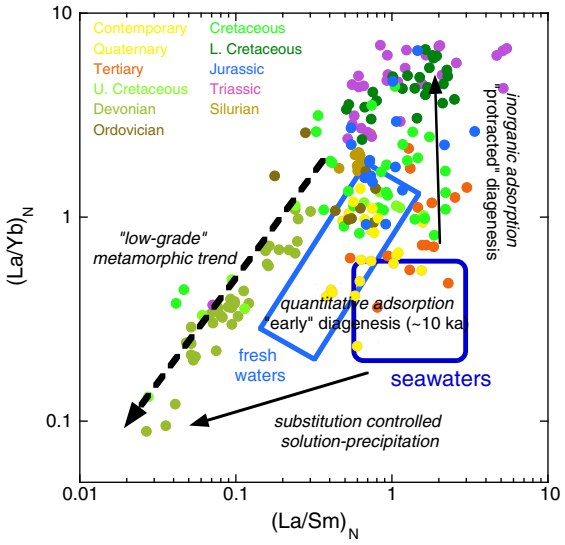

Fig. 11. Observed La/Yb vs. La/Sm ratios in fossil apatites (circles with color scale according to age), and fresh and oceanic waters. Data from: Devonian conodonts (Grandjean-Lécuyer et al., 1993); Silurian conodonts and fish, Bertram et al., 1992; Tertiary and Mesozoic fish (Grandjean et al., 1988; Grandjean, 1989; Grandjean and Albarède, 1989); Quaternary fish (Elderfield and Pagett, 1986); fresh waters: rivers and lakes (Elderfield et al., 1990; Giblin and Dickson, 1992; Johannesson and Lyons, 1995); seawaters include estuarine and coastal waters (Elderfield et al., 1990); oceanic waters 0–4500 m depths (Elderfield et al., 1990; German et al., 1995; Zhang and Nozaki, 1996). The arrows indicate the shifts induced by the fractionation associated with the adsorption — subvertical, and substitution — sub-horizontal mechanisms. Thick dashed line indicates the metamorphic trend. Modified from Reynard et al. (1999).

4.2. Timescales of incorporation and dating

Dating fossils directly by radiochronometric methods is a central problem in archeology and paleontology. Depending on age, different methods can be applied to date to fossil bone and tooth enamel. U-series method applies to samples up to 300 ka in age (Grün et al., 1999), the U/Pb method to samples older than 1 Ma (Balter et al., 2008a,b), and the U/Pb (Fassett et al., 2011) and Lu/Hf (Barfod et al., 2002, 2003, 2005; Kocsis et al., 2010; Herwartz et al., 2011) methods to samples above several Ma in age. Fossil bone or tooth enamel is a non-ideal target for geochronology. The material to be dated should be a clean and closed system, but phosphatic tissues are none of these. For instance, the extensive interactions between bone or tooth and water practically ruled out the use of the K/Ar system because of the high solubility of K and volatility of Ar.

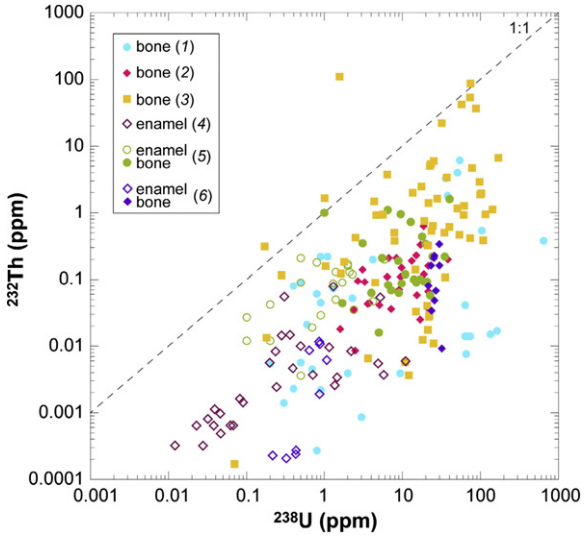

Fig. 12. Correlation of ^{232}Th and ^{238}U concentrations in fossil bone and tooth enamel. Uranium concentration in bone is one order of magnitude higher than for Th, suggesting that U is present both in fossil apatite and in oxy-hydroxides, partly in the form of the labile UO_2^{2+} species. Data from: 1, Pike et al. (2002); 2, Ayliffe and Veeh (1988); 3, Rae et al. (1989); 4, Balter et al. (2008a, 2008b); 5, Esposito et al. (2002); 6, Grün et al. (1999).

Fossil bone and tooth enamel are "dirty" systems, i.e. they contain secondary phases (Kohn et al., 1999), which contribute to parent and/or daughter nuclide concentrations. A compilation of ^{238}U and ^{232}Th shows that their concentrations are correlated in fossil bone and tooth enamel, suggesting that the increase of oxy-hydroxides on which is adsorbed Th contain also U that is added to that of fossil apatite (Fig. 12). Thanks to the different solubility of the apatite and other admixed phases such as calcite and oxy-hydroxides, it is theoretically possible to isolate apatite using leaching technique with dilute acids. This approach has been proposed for more than twenty years for "dirty" calcite such as sedimentary carbonates (Schwarcz and Latham, 1989), but has not systematically been applied to U- and Th-based dating methods in fossil bone and tooth enamel. The precision of the Lu–Hf and Pb–Pb methods was greatly improved by separation of phosphatic material leachates from clays attached to their surface or precipitated within the phosphatic tissue (Barfod et al., 2002).

As discussed earlier, REE patterns reveal the complex sequence of diagenetic alteration in phosphatic remains with associated fractionation and diffusion profiles. Understanding this sequence of diagenetic alteration can provide clues to dating because the radioactive parent is a REE or geochemically similar U. These elements and their decay products enter the bone or tooth almost entirely *post mortem*, with the notable exception of Pb (Curzon and Cutress, 1983; Patterson et al., 1987; Ericson, 2001).

Fossil bone and tooth enamel are open systems that exchange nuclides with the external milieu, picking them up from ambient water and losing them by α-recoil. Diffusion and sequential uptake have been discussed for the distribution of U-series nuclides in fossil bones (Millard and Hedges, 1996; Grün et al., 1999; Kohn, 2008), and a general expression for the open-system production of total ^{206}Pb at secular equilibrium was derived (Balter et al., 2008a,b). Whatever the considered parent–daughter system, the protracted uptake or loss of nuclides leads to younger than "true" or death age. A major breakthrough in dating fossils came from the development of laser ablation technique that allows mapping nuclide concentration and corresponding apparent age (Grün et al., 2008). The state of preservation appears highly heterogeneous within a single tooth and the use of a single parameter U-uptake model can be applied only to well-defined areas.

The ideal case for dating is that of a single, short-lived event of diagenetic uptake of the radiogenic elements. This would correspond for example the early quantitative uptake of REE described above thought to occur within a few ka. At geological timescales, such an event is instantaneous with respect to uncertainties and the obtained ages reflect stratigraphic ages (Barfod et al., 2002, 2003). In the case of archeological material and Quaternary fossils, the diffusion timescale ~1–100 ka may be commensurate with age, and the diffusion and age profiles need to be resolved in order to check that incorporation was achieved in a single-stage (Millard and Hedges, 1996; Grün et al., 2008).

The protracted or multistage intake of REE and radiogenic elements will induce perturbations to the single-stage diffusion profile because concentration changes will be induced with different partitioning, diffusion coefficients, and water compositions leading to the "hat-shaped" REE pattern discussed above (Millard and Hedges, 1996; Grün et al., 2008; Kohn, 2008; Hinz and Kohn, 2010; Kocsis et al., 2010; Trueman et al., 2011). A good example is given by the behavior of the Lu–Hf system, where ages obtained for samples of the Paris–London Mesozoic to Cenozoic basin are in general much younger than stratigraphic age

(by up to several tens of Ma) except in impermeable clay layers (Barfod et al., 2003). Protracted or multistage alteration of REE concentrations and perturbations of Lu–Hf ages in bones and teeth was also documented in other European and North American sedimentary series of similar age (Kocsis et al., 2010; Herwartz et al., 2011). Modeling of REE concentration profiles suggests rapid uptake of TEs, in which case scenarios with several short episodes of uptake have occurred at various times after sedimentation. Lu–Hf dates (Barfod et al., 2003; Kocsis et al., 2010; Herwartz et al., 2011) suggest that the secondary episodes have occurred after the Mesozoic basins were uplifted to a continental setting during Cenozoic, where reopening of phosphatic fossils may progressively take place through variations of water table in aquifers.

For phosphates with the "bell-shaped" patterns, there exists no dating attempts, but it is likely that conodonts from the Montagne Noire (Grandjean-Lécuyer et al., 1993; Girard and Albarède, 1996) would give ages of the low-grade metamorphism associated with Hercynian tectonics of the region.

5. Concluding remarks

Chemical compositions of phosphatic fossils contain information on paleobiological and paleoenvironmental parameters and on diagenetic processes. TE compositions in the living organisms can be understood in terms of ecology, diet and temperature. Thermodynamic modeling of these phenomena should benefit from further experimental investigations and from theoretical studies using atomistic and first-principles calculations. Stable isotope compositions of these "non-traditional" (heavy) elements are nowadays routinely measured by MC-ICP-MS and provide promising lines of development of new geochemical tools for studying diet and metabolism of extinct species. *Post mortem* incorporation of heavy metals such as REE, Th, U could be used to decipher deposition environments and past water chemistry. These compositions are, however, subject to substantial modifications through protracted alteration of phosphatic remains. *Post mortem* TE intake can be used for application in dating deposition if alteration occurred in a single short-duration stage ("early" diagenesis defined by unfractionated REE patterns with respect to environmental waters). It may date opening of the system (e.g. due to aquifer circulation during emersion of sedimentary basins during "protracted" diagenesis), or low-grade metamorphic episode that reset the system via solution–precipitation. These processes are governed by diffusion processes, for which diffusion coefficients differ strongly between estimates from natural, theoretical, and experimental studies.

Acknowledgments

The authors acknowledge CNRS financial support through the INSU programs Eclipse, Eclipse II, Paleo2 and the INEE program EC2CO. Matt Kohn and an anonymous reviewer are thanked for their insightful comments. Several points discussed in this review benefited from discussions with Francis Albarède and Christophe Lécuyer.

References

Albarède, F., Télouk, P., Lamboux, A., Jaouen, K., Balter, V., 2011. Isotopic evidence of unaccounted for Fe and Cu erythropoietic pathways. Metallomics 3, 926–933.
Almora-Barrios, N., Grau-Crespo, R., de Leeuw, N.H., 2013. A computational study of magnesium incorporation in the bulk and surfaces of hydroxyapatite. Langmuir 29, 5851–5856.
Anke, M., Angelow, L., 1995. Rubidium in the food chain. Fresenius J. Anal. Chem. 352, 236–239.
Arrhenius, G., Bramlette, M.N., Picciotto, E., 1957. Localization of radioactive and stable heavy nuclides in ocean sediments. Nature 180, 85–86.
Austin, C., Smith, T.M., Bradman, A., Hinde, K., Joannes-Boyau, R., Bishop, D., Hare, D.J., Doble, P., Eskenazi, B., Arora, M., 2013. Barium distributions in teeth reveal early-life dietary transitions in primates. Nature 498, 216–219.
Ayliffe, L.K., Veeh, H.H., 1988. Uranium-series dating of speleothems and bones from Victoria cave, Naracoorte, South Australia. Chem. Geol. 72, 211–234.
Baig, A.A., Fox, J.L., Wang, Z., Higuchi, W.I., Miller, S.C., Barry, A.M., Otsuka, M., 1999. Metastable equilibrium solubility behavior of bone mineral. Calcif. Tissue Int. 64, 329–339.
Balter, V., 2004. Allometric constraints on Sr/Ca and Ba/Ca partitioning in terrestrial mammalian trophic chains. Oecologia 139, 83–88.
Balter, V., Lécuyer, C., 2004. Determination of Sr and Ba partition coefficients between apatite and water from 5 °C to 60 °C: a potential new thermometer for aquatic paleoenvironments. Geochim. Cosmochim. Acta 68, 423–432.
Balter, V., Lecuyer, C., 2010. Determination of Sr and Ba partition coefficients between apatite from fish (*Sparus aurata*) and seawater: the influence of temperature. Geochim. Cosmochim. Acta 74, 3449–3458.
Balter, V., Reynard, B., 2008. Secondary ionization mass spectrometry imaging of dilute stable strontium labeling in dentin and enamel. Bone 42, 229–234.
Balter, V., Person, A., Labourdette, N., Drucker, D., Renard, M., Vandermeersch, B., 2001. Were Neandertalians essentially carnivores? Sr and Ba preliminary results of the mammalian palaeobiocoenosis of Saint-Cesaire. C. R. Acad. Sci. II 332, 59–65.
Balter, V., Bocherens, H., Person, A., Labourdette, N., Renard, M., Vandermeersch, B., 2002a. Ecological and physiological variability of Sr/Ca and Ba/Ca in mammals of West European mid-Wurmian food webs. Palaeogeogr. Palaeoclimatol. Palaeoecol. 186, 127–143.
Balter, V., Saliege, J.F., Bocherens, H., Person, A., 2002b. Evidence of physico-chemical and isotopic modifications in archaeological bones during controlled acid etching. Archaeometry 44, 329–336.
Balter, V., Blichert-Toft, J., Braga, J., Telouk, P., Thackeray, F., Albarede, F., 2008a. U–Pb dating of fossil enamel from the Swartkrans Pleistocene hominid site, South Africa. Earth Planet. Sci. Lett. 267, 236–246.
Balter, V., Telouk, P., Reynard, B., Braga, J., Thackeray, F., Albarede, F., 2008b. Analysis of coupled Sr/Ca and $^{87}Sr/^{86}Sr$ variations in enamel using laser-ablation tandem quadrupole-multicollector ICPMS. Geochim. Cosmochim. Acta 72, 3980–3990.
Balter, V., Zazzo, A., Moloney, A.P., Moynier, F., Schmidt, O., Monahan, F.J., Albarede, F., 2010. Bodily variability of zinc natural isotope abundances in sheep. Rapid Commun. Mass Spectrom. 24, 605–612.
Balter, V., Lecuyer, C., Barrat, J.A., 2011. Reconstructing seawater Sr/Ca during the last 70 My using fossil fish tooth enamel. Palaeogeogr. Palaeoclimatol. Palaeoecol. 310, 133–138.
Balter, V., Braga, J., Telouk, P., Thackeray, J.F., 2012. Evidence for dietary change but not landscape use in South African early hominins. Nature 489, 558–560.
Balter, V., Lamboux, A., Zazzo, A., Telouk, P., Leverrier, Y., Marvel, J., Moloney, A.P., Monahan, F.J., Schmidt, O., Albarede, F., 2013. Contrasting Cu, Fe, and Zn isotopic patterns in organs and body fluids of mice and sheep, with emphasis on cellular fractionation. Metallomics 5, 1470–1482.
Barfod, G.H., Albarede, F., Knoll, A.H., Xiao, S., Telouk, P., Frei, R., Baker, J.A., 2002. New Lu–Hf and Pb–Pb age constraints on the earliest animal fossils. Earth Planet. Sci. Lett. 201, 203–212.
Barfod, G.H., Otero, O., Albarède, F., 2003. Phosphate Lu–Hf geochronology. Chem. Geol. 200, 241–253.
Barfod, G.H., Krogstad, E.J., Frei, R., Albarède, F., 2005. Lu–Hf and PbSL geochronology of apatites from Proterozoic terranes: a first look at Lu–Hf isotopic closure in metamorphic apatite. Geochim. Cosmochim. Acta 69, 1847–1859.
Bass, J.D., 1995. Elasticity of minerals, glasses, and melts. In: Ahrens, T.J. (Ed.), Mineral Physics and Crystallography. A Handbook of Physical Constants. American Geophysical Union, Washington D.C., pp. 45–63.
Bath, G.E., Thorrold, S.R., Jones, C.M.J., Campana, S.E., McLaren, J., Lam, J.W.H., 2000. Strontium and Barium uptake in aragonitic otoliths of marine fish. Geochim. Cosmochim. Acta 64, 1705–1714.
Bath-Martin, G., Thorrold, S.R., Jones, C.M., 2004. Temperature and salinity effects on strontium incorporation in otoliths of larval spot (*Leiostomus xanthurus*). Can. J. Fish. Aquat. Sci. 61, 34–42.
Bernat, M., 1975. Les isotopes de l'Uranium et du Thorium et les terres rares dans l'environnement marin. Cah. ORSTOM Sér. Géol. 7, 65–83.
Bertram, C.J., Elderfield, H., Aldridge, R.J., Conway Morris, S., 1992. $^{87}Sr/^{86}Sr$, $^{143}Nd/^{144}Nd$ and REEs in Silurian phosphatic fossils. Earth Planet. Sci. Lett. 113, 239–249.
Beyer, G.J., Offord, R., Künzi, G., Aleksandrovska, Y., Ravn, U., Jahn, S., 1997. The influence of EDTMP-concentration on the biodistribution of radio-lanthanides and 225-Acin tumor-bearing mice. Nucl. Med. Biol. 24, 367–372.
Blundy, J.D., Wood, B.J., 1994. On the relationship between elastic moduli and mineral-melt partitioning. Nature 372, 452–454.
Blundy, J., Wood, B., 2003. Partitioning of trace elements between crystals and melts. Earth Planet. Sci. Lett. 210, 383–397.
Brice, J.C., 1975. Some thermodynamic aspects of the growth of strained crystals. J. Cryst. Growth 28, 249–253.
Budd, P., Montgomery, J., Barreiro, B., Thomas, R.G., 2000. Differential diagenesis of strontium in archaeological human dental tissues. Appl. Geochem. 15, 687–694.
Burton, J.H., Price, T.D., 2002. The use and abuse of trace elements for paleodietary research. In: Ambrose, S.H., Katzenberg, M.A. (Eds.), Biogeochemical Approaches to Paleodietary Analysis. Kluwer Academic/Plenum Publishers, New York, pp. 159–171.
Burton, J.H., Price, T.D., Middleton, W.D., 1999. Correlation of bone Ba Ca and Sr Ca due to biological purification of calcium. J. Archaeol. Sci. 26, 609–616.
Campbell, L.M., Fisk, A.T., Wang, X.W., Kock, G., Muir, D.C.G., 2005. Evidence for biomagnification of rubidium in freshwater and marine food webs. Can. J. Fish. Aquat. Sci. 62, 1161–1167.
Cardinal, D., Hamelin, B., Bard, E., Patzold, J., 2001. Sr/Ca, U/Ca and delta O-18 records in recent massive corals from Bermuda: relationships with sea surface temperature. Chem. Geol. 176, 213–233.
Cherniak, D.J., 2000. Rare earth element diffusion in apatite. Geochim. Cosmochim. Acta 64, 3871–3885.

Collins, J.F., Prohaska, J.R., Knutson, M.D., 2010. Metabolic crossroads of iron and copper. Nutr. Rev. 68, 133–147.

Comar, C.L., Russell, R.S., Wasserman, R.H., 1957. Strontium–calcium movement from soil to man. Science 126, 485–492.

Costas-Rodriguez, M., Van Heghe, L., Vanhaecke, F., 2014. Evidence for a possible dietary effect on the isotopic composition of Zn in blood via isotopic analysis of food products by multi-collector ICP-mass spectrometry. Metallomics 6, 139–146.

Crank, J., 1975. The Mathematics of Diffusion. Oxford University Press.

Curzon, M., Cutress, T., 1983. Trace Elements and Dental Disease. PSG Inc., Boston.

Davranche, M., Pourret, O., Gruau, G., Dia, A., Le Coz-Bouhnik, M., 2005. Adsorption of REE(III)-humate complexes onto MnO_2: experimental evidence for cerium anomaly and lanthanide tetrad effect suppression. Geochim. Cosmochim. Acta 69, 4825–4835.

De Baar, H.J.W., Bacon, M.P., Brewer, P.G., 1983. Rare-earth distributions with a positive Ce anomaly in the Western North-Atlantic ocean. Nature 301, 324–327.

De Baar, H.J.W., Bacon, M.P., Brewer, P.G., Bruland, K.W., 1985. Rare-earth elements in the Pacific and Atlantic oceans. Geochim. Cosmochim. Acta 49, 1943–1959.

De Deckker, P., Chivas, A.R., Shelley, J.M.G., 1999. Uptake of Mg and Sr in the euryhaline ostracod *Cyprideis* determined from in vitro experiments. Palaeogeogr. Palaeoclimatol. Palaeoecol. 148, 105–116.

de Villiers, S., Shen, G.T., Nelson, B.K., 1994. The Sr/Ca-temperature relationship in coralline aragonite: influence of variability in $(Sr/Ca)_{seawater}$ and skeletal growth parameters. Geochim. Cosmochim. Acta 58, 197–208.

DeForest, D.K., Brix, K.V., Adams, W.J., 2007. Assessing metal bioaccumulation in aquatic environments: the inverse relationship between bioaccumulation factors, trophic transfer factors and exposure concentration. Aquat. Toxicol. 84, 236–246.

DeNiro, M.J., Epstein, S., 1978. Influence of diet on distribution of carbon isotopes in animals. Geochim. Cosmochim. Acta 42, 495–506.

Dietzel, M., Gussone, N., Eisenhauer, A., 2004. Co-precipitation of Sr^{2+} and Ba^{2+} with aragonite by membrane diffusion of CO_2 between 10 and 50 °C. Chem. Geol. 203, 139–151.

Eary, J.F., Collins, C., Stabin, M., Vernon, C., Petersdorf, S., Baker, M., Hartnett, S., Ferency, S., Addison, S.J., Appelbaum, F., Gordon, E.E., 1993. Samarium-153-EDTMP biodistribution and dosimetry estimation. J. Nucl. Med. 34, 1031–1036.

Elderfield, H., Greaves, M.J., 1982. The rare-earth elements in sea-water. Nature 296, 214–219.

Elderfield, H., Pagett, R., 1986. Rare earth elements in ichthyoliths: variations with redox conditions and depositional environment. Sci. Total Environ. 49, 175–197.

Elderfield, H., Sholkovitz, E.R., 1987. Rare earth elements in the pore waters of reducing nearshore sediments. Earth Planet. Sci. Lett. 82, 280–288.

Elderfield, H., Upstillgoddard, R., Sholkovitz, E.R., 1990. The rare-earth elements in rivers, estuaries, and coastal seas and their significance to the composition of ocean waters. Geochim. Cosmochim. Acta 54, 971–991.

Elias, R.W., Hirao, Y., Patterson, C.C., 1982. The circumvention of the natural biopurification along nutrient pathways by atmospheric inputs of industrial lead. Geochim. Cosmochim. Acta 46, 2561–2580.

Elin, R.J., 1987. Assessment of magnesium status. Clin. Chem. 33, 1965–1970.

Ericson, J.E., 2001. Enamel lead biomarker for prenatal exposure assessment. Environ. Res. A 87, 136–140.

Esposito, M., Reyss, J.L., Chaimanee, Y., Jaeger, J.J., 2002. U-series dating of fossil teeth and carbonates from Snake Cave, Thailand. J. Archaeol. Sci. 29, 341–349.

Ezzo, J.A., 1994. Putting the chemistry back into archaeological bone chemistry analysis — modeling potentials paleodietary indicators. J. Anthropol. Archaeol. 13, 1–34.

Fassett, J.E., Heaman, L.M., Simonetti, A., 2011. Direct U–Pb dating of Cretaceous and Paleocene dinosaur bones, San Juan Basin, New Mexico. Geology 39, 159–162.

Fowler, A.J., Campana, S.E., Jones, C.M., Thorrold, S.R., 1995. Experimental assessment of the effect of temperature and salinity on elemental compositions of otoliths using laser-ablation ICPMS. Can. J. Fish. Aquat. Sci. 52, 1431–1441.

Frank, R.M., Sargentini-Maier, M.L., Turlot, J.C., Leroy, M.J.F., 1989. Zinc and strontium analyses by energy dispersive X-ray fluorescence in human permanent teeth. Arch. Oral Biol. 34, 593–597.

Fujimaki, H., 1986. Partition coefficients of Hf, Zr, and REE between zircon, apatite, and liquid. Contrib. Mineral. Petrol. 94, 42–45.

Fulmer, M.T., Hankermayer, C.R., Constantz, B., Ross, J., 2002. Measurements of the solubilities and dissolution rates of several hydroxyapatites. Biomaterials 23, 751–755.

German, C.R., Masuzawa, T., Greaves, M.J., Elderfield, H., Edmond, J.M., 1995. Dissolved rare earth elements in the Southern Ocean: cerium oxidation and the influence of hydrography. Geochim. Cosmochim. Acta 59, 1551–1558.

Giblin, A.M., Dickson, B.L., 1992. Source, distribution and economic significance of trace elements in groundwaters from Lake Tyrrell, Victoria, Australia. Chem. Geol. 96, 133–149.

Gilbert, C., Sealy, J., Sillen, A., 1994. An investigation of barium, calcium, and strontium as palaeodietary indicators in the southwestern Cape, South Africa. J. Archaeol. Sci. 21, 173–184.

Gilmore, R.S., Katz, J.L., 1982. Elastic properties of apatites. J. Mater. Sci. 17, 1131–1141.

Girard, C., Albarède, F., 1996. Trace elements in conodont phosphates from the Frasnian/Famennian boundary. Palaeogeogr. Palaeoclimatol. Palaeoecol. 126, 195–209.

Gnanapragasam, E.K., Lewis, B.-A., 1995. Elastic strain energy and the distribution coefficient of radium in solid solutions with calcium salts. Geochim. Cosmochim. Acta 59, 5103–5111.

Grandjean, P., 1989. Les terres rares et la composition isotopique du néodyme dans les phosphates biogènes: traceurs des processus paléo-océanographiques et sédimentaires. Institut National Polytechnique de Lorraine Nancy, p. 319.

Grandjean, P., Albarède, F., 1989. Ion probe measurements of rare earth elements in biogenic phosphates. Geochim. Cosmochim. Acta 53, 3179–3183.

Grandjean, P., Cappetta, H., Michard, A., Albarede, F., 1987. The assessment of REE patterns and $^{143}Nd/^{144}Nd$ ratios in fish remains. Earth Planet. Sci. Lett. 84, 181–196.

Grandjean, P., Cappetta, H., Albarède, F., 1988. The REE and ε_{Nd} of 40–70 Ma old fish debris from the West African platform. Geophys. Res. Lett. 15, 389–392.

Grandjean-Lécuyer, P., Feist, R., Albarede, F., 1993. Rare earth elements in old biogenic apatites. Geochim. Cosmochim. Acta 57, 2507–2514.

Gromet, L.P., Dymek, R.F., Haskin, L.A., Korotev, R.L., 1984. The "North american shale composite": its compilation, major and trace element characteristics. Geochim. Cosmochim. Acta 48, 2469–2482.

Grün, R., McCulloch, M.T., Mortimer, G., 1999. Detailed mass spectrometric U-series analyses of two teeth from the archaeological site of Pech de l'Aze II: Implications for uranium migration and dating. J. Archaeol. Sci. 26, 1301–1310.

Grün, R., Aubert, M., Joannes-Boyau, R., Moncel, M.H., 2008. High resolution analysis of uranium and thorium concentration as well as U-series isotope distributions in a Neanderthal tooth from Payre (Ardeche, France) using laser ablation ICP-MS. Geochim. Cosmochim. Acta 72, 5278–5290.

Guidry, M.W., Mackenzie, F.T., 2003. Experimental study of igneous and sedimentary apatite dissolution: control of ph, distance from equilibrium, and temperature on dissolution rates. Geochim. Cosmochim. Acta 67, 2949–2963.

Henderson, P., Marlow, C.A., Molleson, T.I., Williams, C.T., 1983. Patterns of chemical-change during bone fossilization. Nature 306, 358–360.

Herwartz, D., Tütken, T., Münker, C., Jochum, K.P., Stoll, B., Sander, P.M., 2011. Timescales and mechanisms of REE and Hf uptake in fossil bones. Geochim. Cosmochim. Acta 75, 82–105.

Heuser, A., Eisenhauer, A., 2010. A pilot study on the use of natural calcium isotope ((44) ca/Ca-40) fractionation in urine as a proxy for the human body calcium balance. Bone 46, 889–896.

Hildebrand, M., Volcani, B.E., Gassmann, W., Schroeder, J.I., 1997. A gene family of silicon transporters. Nature 385, 688–689.

Hinners, T.A., Hughes, R., Outridge, P.M., Davis, W.J., Simon, K., Woolard, D.R., 1998. Interlaboratory comparison of mass spectrometric methods for lead isotopes and trace elements in NIST SRM 1400 Bone Ash. J. Anal. At. Spectrom. 13, 963–970.

Hinz, E.A., Kohn, M.J., 2010. The effect of tissue structure and soil chemistry on trace element uptake in fossils. Geochim. Cosmochim. Acta 74, 3213–3231.

Hodges, R., MacDonald, N., Nusbaum, R., Staearns, R., Ezmirlian, F., Spain, P., McArthur, C., 1950. The strontium content of human bones. J. Biol. Chem. 185, 519–525.

Holmes, J.M., Davies, D.H., Meath, W.J., Beebe, R.A., 1964. Gas adsorption and surface structure of bone mineral. Biochemistry 3, 2019–2024.

Hotz, K., Krayenbuehl, P.A., Walczyk, T., 2012. Mobilization of storage iron is reflected in the iron isotopic composition of blood in humans. J. Biol. Inorg. Chem. 17, 301–309.

Iolascon, A., De Falco, L., 2009. Mutations in the gene encoding DMT1: clinical presentation treatment. Semin. Hematol. 46, 358–370.

Iyengar, G.V., 1998. Reevaluation of the trace element content in Reference Man. Radiat. Phys. Chem. 51, 545–560.

Jaouen, K., Balter, V., Herrscher, E., Lamboux, A., Telouk, P., Albarede, F., 2012. Fe and Cu stable isotopes in archeological human bones and their relationship to sex. Am. J. Phys. Anthropol. 148, 334–340.

Jaouen, K., Pons, M.L., Balter, V., 2013. Iron, copper and zinc isotopic fractionation up mammal trophic chains. Earth Planet. Sci. Lett. 374, 164–172.

Jemal, M., Ben Cherifa, A., Khattech, I., Ntahomvukiye, 1995. Standard enthalpies of formation and mixing of hydroxy- and fluorapatite. Thermochim. Acta 259, 13–21.

Johannesson, K.H., Lyons, W.B., 1995. Rare-earth element geochemistry of Colour Lake, an acidic freshwater lake on Axel Heiberg Island, Northwest Territories, Canada. Chem. Geol. 119, 209–223.

Kawabata, K., Yamamoto, T., 2010. First-principles calculations of the elastic properties of hydroxyapatite doped with divalent ions. J. Ceram. Soc. Jpn. 118, 548–549.

Kinsmann, D.J.J., Holland, H.D., 1969. The coprecipitation of cations with $CaCO_3$ — IV. The coprecipitation of Sr^{2+} with aragonite between 16 and 96 °C. Geochim. Cosmochim. Acta 33, 1–18.

Kocsis, L., Trueman, C.N., Palmer, M.R., 2010. Protracted diagenetic alteration of REE contents in fossil bioapatites: direct evidence from Lu–Hf isotope systematics. Geochim. Cosmochim. Acta 74, 6077–6092.

Koeppenkastrop, D., De Carlo, E.H., 1992. Sorption of rare earth elements from seawater onto synthetic mineral particles: an experimental approach. Chem. Geol. 95, 251–263.

Kohn, M.J., 2008. Models of diffusion-limited uptake of trace elements in fossils and rates of fossilization. Geochim. Cosmochim. Acta 72, 3758–3770.

Kohn, M.J., Moses, R.J., 2013. Trace element diffusivities in bone rule out simple diffusive uptake during fossilization but explain in vivo uptake and release. Proc. Natl. Acad. Sci. 110, 419–424.

Kohn, M.J., Schoeninger, M.J., Barker, W.W., 1999. Altered states: effects of diagenesis on fossil tooth chemistry. Geochim. Cosmochim. Acta 63, 2737–2747.

Kohn, M.J., Morris, J., Olin, P., 2013. Trace element concentrations in teeth — a modern Idaho baseline with implications for archeometry, forensics, and palaeontology. J. Archaeol. Sci. 40, 1689–1699.

Lea, D.W., Mashiotta, T.A., Spero, H.J., 1999. Controls on magnesium and strontium uptake in planktonic foraminifera determined by live culturing. Geochim. Cosmochim. Acta 63, 2369–2379.

Lecuyer, C., Reynard, B., Grandjean, P., 2004. Rare earth element evolution of Phanerozoic seawater recorded in biogenic apatites. Chem. Geol. 204, 63–102.

Luo, Y., Byrne, R.H., 2004. Carbonate complexation of yttrium and the rare earth elements in natural waters. Geochim. Cosmochim. Acta 68, 691–699.

Lyengar, V., 1989. Elemental analysis of biological systems. Biomedical, Compositional, Environmental and Methodological Aspects. vol. 1. CRC Press, Boca Raton, Fla., USA.

Martin, J.E., Vance, D., Balter, V., 2014. Natural variation of magnesium isotopes in mammal bones and teeth from two South African trophic chains. Geochim. Cosmochim. Acta 130, 12–20.

Mayer, I., Featherstone, J.D.B., 2000. Dissolution studies of Zn-containing carbonated hydroxyapatites. J. Cryst. Growth 219, 98–101.

Millard, A.R., Hedges, R.E.M., 1996. A diffusion–adsorption model of uranium uptake by archaeological bone. Geochim. Cosmochim. Acta 60, 2139–2152.
Nagasawa, H., 1966. Trace element partition coefficient in ionic crystals. Science 152, 767–769.
Nugent, L.J., 1970. Theory of the tetrad effect in the lanthanide(III) and actinide(III) series. J. Inorg. Nucl. Chem. 32, 3485–3491.
Onuma, N., Masuda, F., Hirano, M., Wada, K., 1979. Crystal structure control on trace element partition in molluscan shell formation. Geochem. J. 13, 187–189.
Parker, R.B., Toots, H., 1970. Minor elements in fossil bone. Geol. Soc. Am. Bull. 81, 925–932.
Patterson, C.C., Shirahata, H., Ericson, J.E., 1987. Lead in ancient human bones and its relevance to historical developments of social problems with lead. Sci. Total Environ. 61, 167–200.
Peek, S., Clementz, M.T., 2012. Ontogenetic variations in Sr/Ca and Ba/Ca ratios of dental bioapatites from *Bos taurus* and *Odocoileus virginianus*. J. Trace Elem. Med. Biol. 26, 248–254.
Peppard, D.F., Mason, G.W., Lewey, S., 1969. A tetrad effect in the liquid–liquid extraction ordering of lanthanides(III). J. Inorg. Nucl. Chem. 31, 2271–2272.
Picard, S., Lécuyer, C., Garcia, J.P., Dromart, G., Sheppard, S.M.F., 2002. Rare earth element contents of Jurassic fish and reptile teeth and their potential relation to seawater composition (Anglo-Paris Basin, France and England). Chem. Geol. 186, 1–16.
Pike, A.W.G., Hedges, R.E.M., Van calsteren, P., 2002. U-series dating of bone using the diffusion–adsorption model. Geochim. Cosmochim. Acta 66, 4273–4286.
Plummer, L.N., Busenberg, E., 1987. Thermodynamics of aragonite–strontianite solid solutions: results from stoichiometric solubility at 25 and 76 °C. Geochim. Cosmochim. Acta 54, 1393–1411.
Pourret, O., Davranche, M., Gruau, G., Dia, A., 2007. Competition between humic acid and carbonates for rare earth elements complexation. J. Colloid Interface Sci. 305, 25–31.
Pucéat, E., Reynard, B., Lécuyer, C., 2004. Can crystallinity be used to determine the degree of chemical alteration of biogenic apatites? Chem. Geol. 205, 83–97.
Rabone, J.A.L., De Leeuw, N.H., 2006. Interatomic potential models for natural apatite crystals: incorporating strontium and the lanthanides. J. Comput. Chem. 27, 253–266.
Rae, A., Hedges, R.E.M., Ivanovich, M., 1989. Further studies for uranium-series dating of fossil bone. Appl. Geochem. 4, 331–337.
Rakovan, J., Reeder, R.J., 1996. Intracrystalline rare earth element distributions in apatite: surface structural influences on incorporation during growth. Geochim. Cosmochim. Acta 60, 4435–4445.
Rasmussen, K.L., Boldsen, J.L., Kristensen, H.K., Skytte, L., Hansen, K.L., Molholm, L., Grootes, P.M., Nadeau, M.J., Eriksen, K.M.F., 2008. Mercury levels in Danish Medieval human bones. J. Archaeol. Sci. 35, 2295–2306.
Resche, I., Chatal, J.F., Pecking, A., Ell, P., Duchesne, G., Rubens, R., Fogelman, I., Houston, S., Fauser, A., Fischer, M., Wilkins, D., 1997. A dose-controlled study of ^{153}Sm-ethyldiaminetetramethylenephosphonate (EDTMP) in the treatment of patients with painful bone metastases. Eur. J. Cancer 33, 1583–1591.
Reynard, B., Lecuyer, C., Grandjean, P., 1999. Crystal-chemical controls on rare-earth element concentrations in fossil biogenic apatites and implications for paleoenvironmental reconstructions. Chem. Geol. 155, 233–241.
Reynard, L.M., Henderson, G.M., Hedges, R.E.M., 2010. Calcium isotope ratios in animal and human bone. Geochim. Cosmochim. Acta 74, 3735–3750.
Reynard, L.M., Henderson, G.M., Hedges, R.E.M., 2011. Calcium isotopes in archaeological bones and their relationship to dairy consumption. J. Archaeol. Sci. 38, 657–664.
Reynard, L.M., Pearson, J.A., Henderson, G.M., Hedges, R.E.M., 2013. Calcium isotopes in juvenile milk-consumers. Archaeometry 55, 946–957.
Rimbert, J.N., Kellershohn, C., Dumas, F., Fortier, D., Mazière, M., Hubert, C., 1982. Mössbauer spectroscopy and perturbed angular correlation studies of the rare-and alkaline-earth bone uptake. Biochimie 63, 931–936.
Rosenheim, B.E., Swart, P.K., Thorrold, S.R., Willenz, P., Berry, L., Latkoczy, C., 2004. High-resolution Sr/Ca records in sclerosponges calibrated to temperature in situ. Geology 32, 145–148.
Schrauzer, G.N., 2002. Lithium: occurrence, dietary intakes, nutritional essentiality. J. Am. Coll. Nutr. 21, 14–21.
Schwarcz, H.P., Latham, A.G., 1989. Dirty calcites 1. Uranium-series dating of contaminated calcite using leachates alone. Chem. Geol. Isot. Geosci. 80, 35–43.
Schwarz, K., Milne, D.B., 1972. Growth promoting effects of silicon in rats. Nature 239, 333–334.
Shannon, R.D., 1976. Revised effective ionic radii and systematic studies of interatomic distances in halides and chalcogenides. Acta Crystallogr. A32, 751–757.
Shaw, H.F., Wasserburg, G.J., 1985. Sm–Nd in marine carbonates and phosphates: implications for Nd isotopes in seawater and crustal ages. Geochim. Cosmochim. Acta 49, 503–518.
Shen, C.C., Lee, T., Chen, C.Y., Wang, C.H., Dai, C.F., Li, L.A., 1996. The calibration of D[Sr/Ca] versus sea surface temperature relationship for *Porites* coral. Geochim. Cosmochim. Acta 60, 3849–3858.
Shields, G.A., Webb, G.E., 2004. Has the REE composition of seawater changed over geological time? Chem. Geol. 204, 103–107.
Sinclair, D., Kinsley, L.P.J., McCulloch, M.T., 1998. High resolution analysis of trace elements in corals by laser ablation ICP-MS. Geochim. Cosmochim. Acta 62, 1889–1901.
Skulan, J., DePaolo, D.J., 1999. Calcium isotope fractionation between soft and mineralized tissues as a monitor of calcium use in vertebrates. Proc. Natl. Acad. Sci. U. S. A. 96, 13709–13713.
Skulan, J., Bullen, T., Anbar, A.D., Puzas, J.E., Shackelford, L., LeBlanc, A., Smith, S.M., 2007. Natural calcium isotopic composition of urine as a marker of bone mineral balance. Clin. Chem. 53, 1155–1158.
Sosdian, S.M., Lear, C.H., Tao, K., Grossman, E.L., O'Dea, A., Rosenthal, Y., 2013. Cenozoic seawater Sr/Ca evolution. Geochem. Geophys. Geosyst. 14, 263–264.
Spadaro, J., Becker, R., Bachman, C., 1970. The distribution of trace metal ions in bone and tendon. Calcif. Tissue Res. 6, 49–54.
Sponheimer, M., Lee-Thorp, J.A., 2006. Enamel diagenesis at South African Australopith sites: implications for paleoecological reconstruction with trace elements. Geochim. Cosmochim. Acta 70, 1644–1654.
Stipp, S.L., Hochella Jr., M.F., Parks, G.A., Leckie, J.O., 1992. Cd^{2+} uptake by calcite, solid-state diffusion, and the formation of solid-solution: interface processes observed with near-surface sensitive techniques (XPS, LEED, and AES). Geochim. Cosmochim. Acta 56, 1941–1954.
Stoeltzner, H., 1908. The influence of strontium feeding on the chemical composition of growing bones. Biochem. Z. 12, 119–137.
Stoll, H.M., Rosenthal, Y., Falkowski, P., 2002. Climate proxies from Sr/Ca of coccolith calcite: calibrations from continuous culture of *Emiliania huxleyi*. Geochim. Cosmochim. Acta 66, 927–936.
Suarez, C.A., Suarez, M.B., Terry, D.O., Grandstaff, D.E., 2007. Rare earth element geochemistry and taphonomy of the early Cretaceous Crystal Geyser dinosaur quarry, East-Central Utah. PALAIOS 22, 500–512.
Suarez, C.A., Macpherson, G.L., González, L.A., Grandstaff, D.E., 2010. Heterogeneous rare earth element (REE) patterns and concentrations in a fossil bone: implications for the use of REE in vertebrate taphonomy and fossilization history. Geochim. Cosmochim. Acta 74, 2970–2988.
Trueman, C.N., Tuross, N., 2002. Trace elements in recent and fossil bone apatite. Rev. Mineral. Geochem. 48, 489–521.
Trueman, C.N., Kocsis, L., Palmer, M.R., Dewdney, C., 2011. Fractionation of rare earth elements within bone mineral: a natural cation exchange system. Palaeogeogr. Palaeoclimatol. Palaeoecol. 310, 124–132.
Vidaud, C., Bourgeois, D., Meyer, D., 2012. Bone as target organ for metals: the case of f-elements. Chem. Res. Toxicol. 25, 1161–1175.
Walczyk, T., von Blanckenburg, F., 2002. Natural iron isotope variations in human blood. Science 295, 2065–2066.
Wasserman, R.H., Comar, C.L., Papadopoulou, D., 1957. Dietary calcium levels and retention of radiostrontium in the growing rat. Science 126, 1180–1182.
Wright, J., Seymour, R.S., Shaw, H.F., 1984. REE and Nd isotopes in conodont apatite: variations with geological age and depositionnal environment. In: Clark, D.L. (Ed.), Conodont Biofacies and Provincialism, pp. 325–340.
Yamaguchi, M., Inamoto, K., Suketa, Y., 1986. Effect of essential trace metals on bone metabolism in weanling rats: comparison with zinc and other metals' actions. Res. Exp. Med. 186, 337–342.
Yamaguchi, M., Oishi, H., Suketa, Y., 1987. Stimulatory effect of zinc on bone formation in tissue culture. Biochem. Pharmacol. 36, 4007–4012.
Yi, H., Balan, E., Gervais, C., Segalen, L., Fayon, F., Roche, D., Person, A., Morin, G., Guillaumet, M., Blanchard, M., Lazzeri, M., Babonneau, F., 2013. A carbonate-fluoride defect model for carbonate-rich fluorapatite. Am. Mineral. 98, 1066–1069.
Yuan-Hui, L., Gregory, S., 1974. Diffusion of ions in sea water and in deep-sea sediments. Geochim. Cosmochim. Acta 38, 703–714.
Zacherl, D.C., Paradis, G., Lea, D.W., 2003. Barium and strontium uptake into larval protoconchs and statoliths of the marine neogastropod *Kelletia kelletii*. Geochim. Cosmochim. Acta 67, 4091–4099.
Zhang, J., Nozaki, Y., 1996. Rare earth elements and yttrium in seawater: ICP-MS determinations in the East Caroline, Coral Sea, and South Fiji basins of the western South Pacific Ocean. Geochim. Cosmochim. Acta 60, 4631–4644.